

Thank you to the three reviewers and editor for their suggestions and insightful comments, we have made changes to improve the manuscript and look forward to any further comments.

Editor

1 - Introduction: As mentioned by R3, add a specific statement of a claim(s) of the paper, explicitly mentioning what you show exactly in this paper that help to improve the knowledge of this topic. Also justify at the end of the introduction why you chose these examples, and especially why they are relevant to fluid injection operations as mentioned by R2.

Within the introduction we have added our specific claim of observing three end-member type conceptual models of nonconformities and the testing of the impact of these nonconformity types through the use of hydrogeologic models (65).

We have added justification for the examples presented in this manuscript and their potential relationships to fluid injection operations. (35-45).

We have expanded our synthesis of observations and potential implications for fluid rock interactions (discussion section).

2 - Reorganize the paper and especially add a section on local geology descriptions for each sites, which is mentioned by both reviewers. Also consider if it would be better to place the numerical modelling part in the result section as suggested by R1.

We have added a summary of local geology for each analog site and reformatted figures to support this summary.

We have reorganized portions of the manuscript, moving details about the modelling methods to the methods section and the modelling results to the results section. In the discussion we link the observations made in the nonconformity zone to the model results improving the implications for this work and illustrating the impact of the end-member nonconformity types (I, II, or III).

3 - Better synthesize, hierarchize and organize your observations (avoid listings) as suggested by R1. Highlight the most important observations that are used in the interpretations and better consider them in an applied or global sense in the discussion section.

We reorganized the discussion and made changes recommended by the reviewer.

4 - Better illustrate the fractures, veins and faults with photographs and add more precise descriptions (quantitative if possible) with relevant terminology as mentioned by R2 and R3.

We have improved labeling to illustrate fractures, veins, and faults and added more precise descriptions throughout the manuscript.

5 - Give more information about the lateral variability of the non-conformities as suggested by R2.

We have added greater detail on the lateral variability of nonconformities in outcrop (168 & 191).

6 - Avoid speculation about fluid circulation and diagenesis in the discussion section as mentioned by R3. Intergrate the relevant literature to give support to these interpretations.

We have integrated citations regarding fluid circulation and diagenesis as recommended.

**Reviewer 1:**

Line Item and Technical Comments: 20: Capitalize "Great Unconformity" – change made

24: Perhaps just name the types here, rather than write around them? - change made

26: Which one, and why? What contributes to allowing or inhibiting? – change made

43: Missing second parenthesis. – change made

45: This paragraph outlines the results from this study, but, due to its position in the introduction, makes it sound like a prior observation or known phenomena. I think it either needs more citations, or to be moved later into the intro as part of what you are describing as your work and the results of this study. – re-organized as per R1,R2,R3 comments (55)

60: Whole-rock core here (and in the title) seems a bit redundant. Is this to differentiate between core and cuttings? – change made

73: : : observed/described rock AND fracture and fault features. Without introducing observations of fault/fractures earlier, the descriptions at each site seem to come out of the blue or to be irrelevant to the main hypothesis, even though faults and fractures in the basement are clearly very important. – We have added details earlier in manuscript

77-84: This is a broad site description, not really methods. I would suggest including a more generic section on Geologic Setting (which could include much of what you describe in results), expanding the methods, and streamlining results so the reader can more easily map to your synthesis diagram in Fig. 12.

We have included a brief section (section 2) that describes the geologic setting of each site.

86-87: Analytical methods could be more detailed, or reference details in archived dataset. The specificity of the mineral identification from XRD is impressive, so it would be nice to know what kind of equipment, scan times, and analysis software was used. – Details included.

125: Regarding granular flow, could use citation. – change made

178: "altered and altered" – change made

180: missing a period after (Anderson, 2012) – change made

180-183: This statement would lead naturally to a broader synthesis discussion point about the nature of the nonconformity in mafic, rift-related portions of the midcontinent.

This statement has been incorporated into the geologic setting and used in synthesis within the discussion.

183: Looks like a missing space after “1995).”? – change made

192: The paragraph break here is confusing for me, as the topic sentence is about the Mt. Simon, but the next few sentences are again referring to the altered upper portion of the basement, but that is not entirely clear until the reference to “50 m zone: :” – added clarification

199: Either new sentence or semi-colon at “contact, locally: :” – change made

223: The observation that the altered shear zone can be fractured/reactivated would be another point to include in a broader synthesis: zones of prior deformation are more likely to be zones of subsequent deformation –

**Noted. We have revised discussion to synthesize observations more clearly.**

229: Another good point to fold into a broader synthesis: phyllosilicates at the contact may inhibit cross-nonconformity fractures and flow, but maybe need to discuss their origin.

**Noted. We have revised discussion to synthesize observations more clearly in discussion**

225-242: I find this section somewhat confusing. Doesn't the alteration and mineralization suggest fairly extensive fluid-rock interaction? I think the part that is missing is the point that prior fluid rock interaction and alteration has resulted in low permeability now, so perhaps clearing up the temporal aspects? However, mineralization (presumably strengthening) and alteration to phyllosilicates (presumably weakening) are both called upon to act as hydrologic and mechanical barriers, and as written it is hard to understand why. Consider, for instance, the impact of more brittle layers in fault systems (e.g. Schöpfer, M. P. J., Childs, C., & Walsh, J. J. (2006). Localisation of normal faults in multilayer sequences. *Journal of Structural Geology*, 28(5), 816-833. 10.1016/j.jsg.2006.02.003)

Schopfer and other workers (Ferrill et al , Petrie et al, Larsen, Sibson, and others) show the change in failure mode across boundaries, our observation is that under the conditions in which the observed open-mode fractures formed they did not penetrate the nonconformity, reducing a potential future fluid flow pathway, and we expect the difference in relative permeability between the altered boundary and overlying sed. protolith injected fluids would move along the nonconformity. We have reworded this section to clarify.

259: “Our collective field and core observations document the occurrence of significant lateral variations in altered or mineralized zones that are associated with a relatively wide range of permeability values, and that alteration coupled with abundant structural discontinuities can result in relatively higher permeability that extends for 10's of m's both laterally and vertically into the crystalline basement rock below the nonconformity.” Yes, but what controls the variations, and how might someone know from the surface, prior to siting an injection well, if basement faults in a region are more or less likely to be reactivated due to hydrologic properties at the non-conformity? This is the type of synthesis I would

really like to see spelled out more explicitly, even if speculative, and there are sections where you already briefly bring up points that could feed into this broader synthesis (see above).

We have provided clarification and edited the text; other reviewers have requested that we not speculate.

264: Modelling work could be a new method and result, then folded into discussion and used to support your summary diagram in Fig. 12, rather than added to the end. As it is, I find it hard to tell if this is new work, or prior work from J. Ortiz

We have reorganized the inclusion of the modeling work, models were built based on observations presented in this manuscript and have been presented in part by previous work by Ortiz. The models serve to test the impact changing characteristics of the nonconformity have on fluid pressure migration.

267: Note different style “x” shown for “times” in permeability values. Also, is the relative  $z/k_x$  and absolute  $k_z$  shown meant to be for the fault in basement or in the aquifer, because wouldn't at least one of those values need to be different for the two portions of the faults?

We fixed the  $x$ ; and permeability values are different ( $k_x = k_z = 3 \times 10^{-17} \text{ m}^2$ ) in crystalline basement rock vs. conduit-barrier fault ( $k_z/k_x=105$ ;  $k_z = 3 \times 10^{-10} \text{ m}^2$ )

271: Ok, so in this model the low permeability zone formed after the fault? Or was it a weathered horizon that was incorporated into the fault? I wonder because that helps me think about the environment of formation of this zone, which could be very widespread at non-conformities (e.g. soil profiles like Walter et al. (2018) Petrophysical and mineralogical evolution of weathered crystalline basement in western Uganda: Implications for fluid transfer and storage. AAPG Bulletin).

The fault cuts low permeability zones creating a potential permeability pathway.

283: I would like to see these geologic conditions spelled out more explicitly rather than leaving it to the reader to infer them. - revised

284-286: In what scenario would they do both, either? This sentence could be more specific. - revised

288: Do you mean Type 0 and Type 2? I thought Type 1 resulted in reduced fluid communication into the fault zone (line 274-275)?

The faults cutting Type 1 appear to be potential permeability pathways.

295: Shameless plug about impact of fluid chemistry on deformation in mineralized fault rocks, but there are many others too: Callahan, O. A., Eichhubl, P., Olson, J. E., & Davatzes, N. C. (2020). Experimental investigation of chemically aided fracture growth in silicified fault rocks. *Geothermics*, 83. <https://www.doi.org/10.1016/j.geothermics.2019.101724> 359: Looks like a citation manager software glitch. - included

363, 364: Incomplete references? No pages or publisher? Might just be a reference style thing. 385/Figure 1. In legend, using a grey gradient box for 'craton' would be a bit clearer than the current black line, although this may be a reproduction issue.

We have modified the Basemap Figure (Figure 1) to support the newly added geologic setting details.

390/Figure 2. Missing a description of inset “A”. Not clear what diagonal lines are in B, Fault? Dike? Caption could be more informative, for instance noting evidence for fluid-rock interactions in “C”. Some shorthand in captions is confusing, such as “min. congl”. Mineralized? Minimal? - **change made**

395/Figure 3. References to insets change from 1) , 2) to B), C), : : : “Colloform mineralization” image (“C”) is either missing or does not show colloform habit very clearly. What are red lines near 4 and 5 on the “Lithology” log? Why does the thickness start with 0 below weathered basement and not at the non-conformity?

We modified scale, added text to explain Fe mineralization.

397/Figure 4. Could use more descriptive text, for instance, insets A, B, are not discussed. Red arrows in B, C are not described. Fault in C would be easier to see if white or other light color. B would benefit from a scale. – **change made**

400/Figure 5. Choice of height scale at 1.2 m is a bit odd, and “Thickness” may be the wrong word to use here. Maybe depth relative to non-conformity and start with 0 there? Is Espiritu \_10 m thick, or 10.9-9.6 m thick? Because it shows very little, the “Elemental Analysis” column is a bit frustrating. Why not show XRD results as in Figures 3 and 7? Or better yet in all figures with similar columns show alteration/mineralization reactions and products, which could reflect either XRD or elemental work (e.g. + calcite, + albite, -quartz: : :) if you have a mixed bag of analyses. Note typo in 4a “phyllosicilate”. In caption: Espiritu or Espiritu? –

We fixed spelling of Espiritu, changed scale on column, and added explanation of “thickness”.

408/Figure 6: This caption has a lot of passive voice. Unclear to me if the nonconformity is cut by “throughgoing veins” (check typo there) or the veins cut the shear zone, but those scenarios have pretty different implications. – **changes made to clarify text**

414/Figure 7: Perhaps worth noting whether units are measured depth, relative to sea level, true vertical depth, etc. for clarity. – **change made**

425/Figure 8. Typo: “Granitiod” in A. “Pinkcoated” is not particularly helpful; perhaps ID the mineral, even if speculative, or just call them partially-mineralized, sealed, or stained fractures, etc. whatever the case may be. – **change made**

430/Figure 9. Same comment about measured depth for clarity. – **change made**

435/Figure 10. Cool plot. The “Depth” axis on the permeability column is perhaps redundant.

We have kept the depth axis for consistency between the two sub-figures.

444/Figure 11. Photomicrograph 2. What does “intensely weathered \_60 m” mean? Consider argillic alteration or just argillization. Argillite is a rock type, not the product

of argillic alteration. “Iron” capitalized in caption.

Correction to figure text and changes made to figure caption.

446/Figure 12: :. “Phyllosilicate” (in figure) vs “weathering” in caption. What is the rationale for the circular flow path? – change made

R3

The Discussion presents some inferences about fluid circulation and the interpretations of structures and mineral deposits. As it stands some of this text seems speculative. The arguments should at least be bolstered by pointing to some of the extant structural diagenesis literature.

We have added citations to the fracture and diagenesis literature when discussing mineralogic changes.

Where the text describes ‘fractures’ and fracture mineralization, the descriptions could be more complete (and meaningful). More information could be provided on whether the fractures are ‘opening mode’ or faults. The use of the term ‘vein’ is unhelpful, particularly with respect to structures in the cover above the nonconformities. Mineral fill in fractures is common throughout sedimentary sequences (e.g. Laubach et al. 2019, Reviews of Geophysics) and such mineral deposits could provide evidence of the post depositional structural and fluid history of these zones. So a more meaningful description of these features could be useful. Note also that there are a number of published studies of fracture systems in basal Cambrian and in Ordovician sandstones of the midcontinent and other Laurentia cover rocks, and the fracture sets have a range of ages and origins.

We have provided specific descriptions of fracture types throughout and made call outs where possible in figures to identify the features.

Some statement as to how representative these outcrops are of the midcontinent nonconformity zones would be helpful.

We have added a statement on the midcontinent nonconformity study locations and their use as analogs (section 2).

45 I think I follow what you are saying here about the definition of the ‘nonconformity zone’, but perhaps the definition could use sharpening. Are you talking about some volume of rock near the nonconformity that is somehow altered from what it would be if the same rock was not near the nonconformity? Do you only mean rocks in the basement or could this include rocks above the nonconformity? Can you try to make the definition more explicit?

The nonconformity zone is the volume of rock adjacent to the nonconformity, in most cases it is altered, we have clarified this definition (53).

60 Where you mention ‘the nonconformity’ it might help reader if you remind them here that you mean ‘the nonconformity in the US midcontinent region’. – Change made

67 The Introduction would be improved by adding an explicit claim here that could start with the statement 'here we show that: : ': Motivate the reader rather than just providing a list of what you did. – added

68 But are these overlying rocks mostly quartz-rich sandstones? Isn't the basal Cambrian sandstone pretty common? I see that you outline the geology you looked at in section 2.1. Do you discuss how representative these might be? –

We have added this information to Section 2 – Geologic setting.

70 Where in the Introduction do you alert the reader that you present modeling?

We have added reference to modeling into the introduction (77).

86 'detailed' is vague; can you replace this statement with a scale (or range of scales)? Or just omit, since the resolution level is implied by the instruments you used. – change made

90 Is there a reason for the order that you describe the localities? Same question for the listing in section 2.1. A representative selection?

Localities were grouped based on study and sampling sites being outcrop vs core. There is no specific order but the sites are a representative selection of the basement tectonic zones of US mid-continent. We have further addressed this in section 2.

95 How low is the porosity?

We have removed reference to porosity, as at this point in time it is only a qualitative observation from petrography.

100 if the fractures are bedding parallel as you say, it would be hard for them to extend into basement. Or do you mean the reduction spots are not in basement? – reworded sentence

101 Are these slip surfaces in basement subparallel to the bedding parallel 'fractures' in the cover. Are the cover fractures faults?

There is no evidence of slip observed in the bleached fractures in the Jacobsville unit. Evidence of slip was observed in the basement and align with the near-vertical bleached fractures in the cover.

110 By 'span the contact' do you mean the faults extend into the cover? – yes – reworded (184)

115 Something is awkward in the phrasing here. – reworded typo

130 Are you saying fault rock is only found in faults? Clarify text. – change made (line214)

144 Quartz lined and quartz-filled fractures are common in quartzose sandstones even distant from nonconformities. The mineral deposits may not necessarily represent mineralization 'events' since the fractures themselves are reactive surfaces (e.g. Lander and Laubach 2015, GSA Bulletin). – reworded

155 and preceding text. What kind of 'fractures'; opening mode, or faults? Are there crosscutting relations here that provide evidence for the relative timing of these structures? Are you implying that the shear zone in the basement is somehow related to the fractures in the cover? (Wouldn't that be surprising?) – changes made (225>)

165 Is this the porosity range at the site you sampled? It seems a stretch to say that this is the range for the Mt Simon generally, since porosity ought to reflect thermal exposure/burial history and that could vary regionally. Clarify.- reworded

183 space – change made

186 'multi-layered veins and/or fracture mineralization'; are these different things? – reworded

192 'porous'; but can you specify how porous? –

The porosity is qualitative based on petrographic observation at this time. No quantitative estimate of porosity was made and thus we have adjusted text.

197 'structural discontinuities' seems vague. We use this word because it encompasses all types of fractures, veins, faults across all study sites.

203 Is the thickness of the nonconformity zone specified at the outset of each description above? And how did you decide where the boundaries of the zones are? – added improved definition of the nonconformity zone

203 What is the opposite of 'in situ' mineral growth? – change made

206 Maybe put in a table? And refer to in description. – change made

201 The first paragraph of the Discussion seems vague and disorganized. Are these structures in the nonconformity zone' or in the basement or the cover? Are these only 'small faults' or are some of the fractures opening mode? - Discussion has been rewritten for clarity

209 The 'non fractured'; do you mean that these zones lack fractures in general, or that in areas where fractures happen to be absent, the host rock attributes might have these effects? – fractures are absent – reworded for clarity

210 'we note that: : :'; what is the basis for this inference? That there are porous rocks above the basement rocks? -removed statement

219-220 I don't see how it follows that the 'vein mineralogy' provides evidence for cross unconformity flow. Are you talking about mineral filled fractures in the basement or in the cover? Note that from mineral composition alone it can be challenging to find evidence for fluid flow (see for example, Denny et al.2020 GSA Bulletin). Maybe this point needs more development or the conclusion should be presented in a more nuanced way. – reworded

We see consistent mineralized fractures (vein) and cross-cutting relationships within the veins in the basement and sedimentary cover suggesting similar fluid rock interactions.



226 In the older rock mechanics literature there are examples of fracture systems in basement associated in typical midcontinent crystalline rocks that extend to depths of hundreds of meters and then abruptly stop; so zones of penetration of alteration could be much more than 5 m (and might be heterogeneous, if linked to deep seated fractures). See references by Aubertin. – reworded

The sentence was reworded to reflect our direct observations (5 m) and those of previous workers Duffin.

226 ‘that impacts’ or ‘that would be expected to impact’? – change made

236 But are these the ‘bed parallel’ fractures? –

These are fractures that cut across the nonconformity at an angle, so no, not bed-parallel

239 What do you mean by ‘deep circulation’? The basement rocks are not all that far from porous sedimentary rocks, which likely contain fluids.

Change made to avoid confusion. We were referring to ‘deep’ as in basement involved and not limited to circulation within the sedimentary rocks.

241 Where did you mention what the mechanical properties of these rocks is? Did you measure them, or is that an inference from the rock types? An example of mechanical properties inhibiting fracture in the setting you are concerned with is in Ellis et al. 2012, J. Geol. Soc. London. –

No mechanical properties were measured in this work. We have added a citation to support importance of rheology/mechanical change across boundary.

255 do you mean ‘faults’?

Structural discontinuities in this paper could include veins, joints, faults, and cataclastite zones.

259-264 Is this your claim? - reworded

265 Is this modeling work prefigured in the Introduction?

We have added reference to modeling work in introduction.

282 How representative are these various types you identify?

We provide a supplementary table with additional nonconformity sites (7 outcrop sites, 6 core total) at all sites the nonconformities fall into one of the three end-members. We have added text to the conclusion to reference supplementary table and representative nature of these end-members.

303 ‘Laubach’ is the correct spelling. – change made

R2

1. Illustrations of the fractures. The figures largely focus on the petrographic features

and I found that the fracturing mentioned in several places is not fully illustrated. This includes, for example, (1) the near-vertical to bedding-parallel bleached fractures (l.100), (2) basement-hosted slip surfaces (l.101), cm- to m's - displacement faults (l.115), slip surfaces with oblique to dip-slip slickenlines mm's to cm's thick (l.189). . . . I think the manuscript will be improved by illustrating these features. –

**We have added labels on images where possible and have provided references to work done in MS theses.**

2. Lateral variability. Nonconformity zones likely have properties that are spatially heterogeneous. This is indicated l.49-52: “Due to weathering, deformation, diagenesis and fluid-rock interactions, the nonconformity zone may be hydraulically heterogeneous at the mm to 10's m scales”. The paper addresses the vertical variability, but it does not fully address the lateral variability, which is critical for fluid flow and can give insights into how core data can be extrapolated to large-scale application. The studied outcrops allow analysing this lateral variability. For example, rocks studied in section 2.2.2 are observed along a 4-km long section in Gallinas Canyon. I will recommend the authors to further this point. **-change made - added detail**

3. Geological settings. The description of the geological setting is very sparse. I recommend the authors to provide more information for each studied area. For example, the types and ages of the fractures and some general descriptions on the tectonic setting. Maybe providing the locations of the studied areas on geological maps could be useful.

**We. have added a section on geologic setting with locations on maps.**

4. Analogues. Two outcrops are examined: (1) a nonconformity between late Proterozoic Jacobsville Sandstone and early Proterozoic altered peridotite outcropping in Michigan and (2) the contact between Devonian to Mississippian carbonate and clastic rocks of the Espiritu Santo Formation deposited on the Proterozoic quartzofeldspathic and amphibolitic gneiss. Also, three cores are examined: (1) a core recovered from the Cambrian Lamotte Formation sandstone and sheared Proterozoic granitoids in southcentral Nebraska, (2) from the Cambrian Mt. Simon Sandstone and Precambrian altered granitoid gneiss of the Grenville Front Tectonic Zone and (3) from a section of rocks of lower Cambrian Mt Simon Sandstone overlying a Precambrian layered intrusive complex. I think it is interesting to analyse these very different areas because it provides an idea about the diversity of the nonconformity. However, the negative point is that it is not clear whether the studied areas are analogues to fluid injection sites or not. For example, in the introduction, the authors mentioned the mid-continent United States and the works by Murray (2015). This work concerns Oklahoma's underground injections, where target rocks are mostly carbonates from the Arbuckle sedimentary strata above a crystalline basement. My knowledge of the regional geology of the studied areas is limited, but I think it will be worthy to justify the choice of the studied areas and how these areas are relevant for fluid injection operations. I think the last conclusion point: “the contact . . . should instead be evaluated on a site by site basis prior to injection of large fluid volumes” is critical in this regard.

We have added a statement regarding the choice of localities, and how they serve as analogues, the use of Oklahoma as one example of deep injection and associated earthquakes is meant to provide the reader with the research driver that deep injection into reservoirs above the nonconformity has led to earthquakes in crystalline basement –

5. Quantitative insights. The authors briefly describe permeability values measured for one core in section 2.2.4. This is important data and the results could be described further. Besides, I think it could be interesting to provide similar information from the other studied areas. Also, there is a mention of fractures with density decreasing with depth (l.189). I think this could be described quantitatively as well. For example, by providing a fracture density log. More generally I think providing further quantitative analysis will be welcome and will make this work more valuable.

We have added fracture data where possible and have provided references to work done in MS theses.

6. Numerical modelling. I think the last paragraph of the discussion on numerical modelling will be better in the result section. Also, I think that the authors should provide more information about their methodology, the origin of the permeability values, the choice of the studied geometry and the boundary conditions.

We have moved the numerical modelling results to improve flow of the discussion.

Minor points

Mt. Simon or Mount Simon, both are used in the manuscript. – **change made**

2. l.204 “not the result of alteration due to weathering alone”. I think this should be discussed further. – **expanded explanation**

3. The figure captions are often incomplete. – **figure captions edited for completeness**

4. Fig.2: What is A in the figure. There is no scale in B and C. – **fixed typo**

5. Fig. 3. There are no B, C and D in Fig. 3. I think the authors mean 4, 5 and 6. -**change made**  
Although there is no 6 in the figure?

6. Fig. 4: What is A, B and C. There is no scale in B. – **10 cm scale bar appears at bottom of core box photo**

7. Fig. 6: B is not indicated in the caption.- **added callout in caption**

# Geologic characterization of nonconformities using outcrop and core analogues: hydrologic implications for injection-induced seismicity

Elizabeth S. Petrie<sup>1</sup>, Kelly K. Bradbury<sup>2</sup>, Laura Cuccio<sup>2</sup>, Kayla Smith<sup>2</sup>, James P. Evans<sup>2</sup>, John P. Ortiz<sup>4,5</sup>,  
5 Kellie Kerner<sup>3</sup>, Mark Person<sup>3</sup>, and Peter Mozley<sup>3</sup>

<sup>1</sup>Western Colorado University, Geology Department, 1 Western Way, Gunnison, 81231, USA

<sup>2</sup>Utah State University, Geology Department, 4505 Old Main Hill, Logan, UT 84322-4505, USA

<sup>3</sup>New Mexico Institute of Mining and Technology, 801 Leroy Pl Socorro, NM 87801, USA

10 <sup>4</sup>Computational Earth Science Group, Los Alamos National Laboratory, Los Alamos, NM 87544, USA

<sup>5</sup>Johns Hopkins University, Department of Environmental Health and Engineering, 3400 N. Charles St., Baltimore, MD 21218,  
USA

*Correspondence to:* Elizabeth S. Petrie (epetrie@western.edu)

**Abstract.** The occurrence of induced earthquakes in crystalline rocks kilometres from deep wastewater injection wells poses  
15 questions about the influence nonconformity contacts have on the downward and lateral transmission of pore fluid pressure  
and poroelastic stresses. We hypothesize that structural and mineralogical heterogeneities at the sedimentary-crystalline rock  
nonconformity control the degree to which fluids, fluid pressure, and associated poroelastic stresses are transmitted over long  
distances across and along the nonconformity boundary. We examined the spatial distribution of physical and chemical  
heterogeneities in outcrops and ~~whole rock~~ core samples of the ~~great~~-Great Unconformity in the midcontinent of the  
20 United States, capturing a range of tectonic settings and rock properties that we use to characterize the degree of historical  
fluid communication and the potential for future communication. We identify three end-member nonconformity types that  
represent a range of properties that will influence direct fluid pressure transmission and poroelastic responses far from the  
injection site. These nonconformity types vary depending on whether the contact is sharp and minimally altered (*Type 0*), ~~or~~  
~~if it is~~ dominated by phyllosilicates (*Type I*), or secondary non-phyllosilicate mineralization (*Type II*). **We expect the rock**  
25 **properties associated with the presence or absence of secondary non-phyllosilicate mineralization and phyllosilicates to**  
**either allow or inhibit fractures to cross the nonconformity respectively, thus impacting the permeability of the nonconformity**  
**zone.** Our observations provide geologic constraints for modelling fluid migration and the associated pressure communication  
and poroelastic effects at large-scale disposal projects by providing relevant subsurface properties and much needed data  
regarding common alteration minerals that may interact readily with brines or reactive fluids.

30

Formatted: Highlight

Formatted: Highlight

## 1 Introduction

Deep wastewater injection near the nonconformity between the Phanerozoic sedimentary sequence and Proterozoic crystalline basement in the ~~mid-continent~~midcontinent United States (Sloss, 1963) is the primary means by which produced formation fluids are disposed of in Class II injection wells (Murray, 2015). Increased rates of seismicity in this region are associated with large volumes of wastewater injection (Ellsworth et al., 2015; Keranen et al., 2013; Nicholson and Wesson, 1990; Petersen et al., 2016; Zhang et al., 2013), reduction of friction on pre-existing faults, and pressure diffusion away from the injection point controlled by the permeability structure of the rocks in the subsurface (Goebel and Brodsky, 2018; Yehya et al., 2018). Recent ~~mid-continent~~midcontinent seismicity nucleates on faults in crystalline rocks km's from injection sites (Keranen et al., 2014; Weingarten et al., 2015; Zhang et al., 2016), and spans timescales of months to years' post-injection, indicating that pore-fluid pressures and/or poroelastic loads are transmitted across or along the nonconformity ~~zone~~or through connected fracture systems in the crystalline rocks (Ortiz et al., 2019). The depths of seismicity (up to 11 km) at some injection sites suggest that crystalline basement permeability is perhaps moderate to high ( $10^{-16}$  to  $10^{-14}$  m<sup>2</sup>); (Zhang et al., 2016) and is dynamically increased by elevated fluid pressures (Rojstaczer, 2008). Observations presented in this paper are also relevant to Class VI injection wells used for geologic sequestration of CO<sub>2</sub>, several of our analogue sites include deep reservoirs being evaluated for CO<sub>2</sub> sequestration (Leetaru et al., 2009; Leetaru and McBride, 2009; Plains CO<sub>2</sub> Reduction (PCOR) Partnership, 2020; Thorleifson, 2008).

Numerical modelling of fluid flow and/or loading stresses associated with poroelastic effects across nonconformities indicate that: 1) the presence of a high-storativity, low-permeability basal seal reduces potential for basement induced earthquakes; 2) poroelastic effects can trigger seismicity far away from the injection location; 3) the presence of conductive faults, including those that cut the nonconformity and those that are isolated in the basement can provide direct fluid or fluid pressure pathways, and 4) permeable cross-nonconformity faults may exhibit high rates of seismicity (Chang and Segall, 2016; Goebel and Brodsky, 2018; Ortiz et al., 2019; Yehya et al., 2018; Zhang et al., 2013).

In this paper we summarize geologic observations made at the ~~The~~ nonconformity ~~zone is~~zone, ~~the~~ altered rock volume surrounding the nonconformable contact, this zone varies in thickness and is defined by mineralogic and structural alteration of the protolith rocks above and below the nonconformity. ~~nonconformities~~We characterize nonconformity zones that are associated with Precambrian granite, gabbro, gneiss, and schists, ~~and that~~ are overlain by porous sedimentary rocks including sandstone and mixed carbonate-clastic sequences. Study locations were chosen based on their distribution within the midcontinent region and the lithologies present (Figure 1). These analogues represent the diversity of the nonconformity in the United States midcontinent region and are analogues for deep fluid injection from produced waters (Class II) and sequestration of CO<sub>2</sub> (Class VI). At each site we document the lithology and structural features of the rocks on either side of the nonconformity to characterize the range of rock types associated with the contact and identify any evidence of past cross-contact fluid flow. We present data on the mineralogic and structural heterogeneities observed in outcrop and core, and these

Field Code Changed

Field Code Changed

Field Code Changed

Field Code Changed

Field Code Changed

Field Code Changed

Field Code Changed

Field Code Changed

Formatted: Subscript

Formatted: Subscript

Field Code Changed

Formatted: Not Superscript/ Subscript

observations serve as proxies for variation in mineral alteration and deformation at the nonconformity which may impact the future migration of fluids along and across the contact.

The sites evaluated here provide geological and hydrogeological analogues that aid in understanding controls on cross-contact fluid flow and the impacts deep circulating fluids may have on altering rock properties at depth (Oliver et al., 2006). We find three end member types of nonconformity. These zones may range from diffuse to sharp (Type 0), becan be phyllosilicate rich (Type I), or dominated by non-phyllosilicate secondary minerals (Type II). Each contact type observed in this study has a range of mineralized textures and structural discontinuities. Due to weathering, deformation, diagenesis and fluid-rock interactions, the nonconformity zone may be hydraulically heterogeneous at the mm to 10's m scales and influence the migration of fluid and fluid pressures away from the injection well. Characterizing variations in rock properties at the nonconformity zone is critical for safe implementation of deep fluid injection, as the dimensions and hydraulic properties of the rocks in the nonconformity zones impact the subsurface flow regimes (Ortiz et al., 2019). The lithologic character of the nonconformity zone has implications for hydraulically connected regions by allowing direct fluid communication, changes in pore fluid pressure, and/or poroelastic loads.

Because pressure diffusion and fluid migration depend on the permeability structure at a given location, our work can be used to improve hydrogeologic models that test the impact of lithologic changes and cross-nonconformity fractures on the transmission of pore fluids and/or poroelastic stress. We present results from hydrogeologic models based on observations of nonconformity zone characteristics, testing the impact various nonconformity zone types have on transmission of pore fluids.

## 2 Geologic setting

The North American craton, Laurentia, includes the Precambrian shields, the platforms and basins of the North American interior and the reactivated Cordilleran foreland of the southwestern United States (Fig. 1). The craton is composed of includes Archean blocks, the Yavapai-Mazatzal, and Grenville accretionary belts, and failed rifts (Hoffman, 1988; Marshak et al., 2017; Whitmeyer and Karlstrom, 2007). Precambrian exhumation produced erosional surfaces on the top of the crystalline basement which was/were buried by Phanerozoic clastic wedge and marine sedimentary rocks (Marshak et al., 2017; Sloss, 1988). The nonconformities studied in this paper are located within the Superior craton, an Archean basement complex of granite-greenstone or higher grade equivalent overlain by erosional remnants of Early Proterozoic platform facies (Hoffman, 1988), the Yavapai-Mazatzal province, 1.76–1.65 Ga juvenile arc terrane that includes the Central Plains orogeny (Karlstrom and Humphreys, 1998; Sims, 1990; Sims and Peterman, 1986), the Grenville province, 1.3–1.0 Ga imbricate thrust slices formed during continent-continent collision (Rivers, 1997) and the Midcontinent/Midcontinental Rift, ~1.1 Ga failed rift system, dominated by volcanic rocks and basin fill sedimentary rocks, mostly subaerial plateau basalts (Ojakangas et al., 2001) (Figure Fig. 1).

Field Code Changed

Formatted: Line spacing: 1.5 lines

Field Code Changed

Field Code Changed

Formatted: Not Highlight

Formatted: Font: Not Italic

Formatted: Not Highlight

Formatted: Not Highlight

Formatted: Not Highlight

Formatted: Font: Not Italic

Formatted: Font: TimesLTMM\_1\_1000

Formatted: Font: Not Italic

Formatted: Font: Not Italic

Formatted: Font: Not Italic

Formatted: Font: Not Italic

Formatted: Font: Not Italic

Formatted: Font: Not Italic

Formatted: Font: Not Italic

Formatted: Font: TimesLTMM\_1\_1000

Formatted: Font: Not Italic

Formatted: Font: (Default) Times New Roman, Not Italic, English (United Kingdom)

## 2.1 Study areas

### 2.1.1 Outcrop locations:

Exposed at Presque Isle and Hidden Beach along the southern shore of Lake Superior, Michigan the nonconformity is defined by Proterozoic Jacobsville Sandstone overlying early Proterozoic altered peridotite crystalline basement (Figure Fig. 2). At the study localities the Jacobsville Sandstone (Hamblin, 1958) consists of a variably indurated pebble to cobble conglomerate and a lenticular planar to cross-bedded light red quartz arenite (Fig. 2). The geologic history of the Presque Isle serpentinized peridotite is not well constrained. Early research by Wadsworth (1884) believed that the peridotite intruded into Paleozoic sandstone, however, fragments of oxidized peridotite within the Jacobsville Sandstone were reported by Van Hise and Bayley in 1897 and it is thought that the . The current consensus is that the Presque Isle peridotite serpentinized at the between 1.80-1.1 Ga (Gair and Thaden, 1968). The overlying Jacobsville Sandstone is a dominantly fluvial sequence of feldspathic and quartzose sandstones (Malone et al., 2016), and at the study localities consists of a variably indurated pebble to cobble conglomerate and a lenticular planar to cross-bedded light red quartz arenite (Fig. 2). The Presque Isle outcrops are analogues for geologic sequestration of CO<sub>2</sub> in the deep saline Jacobsville Sandstone reservoir (Leetaru and McBride, 2009).

The nonconformity at Gallinas Canyon is exposed along a 4-km long section in the southern-most Sangre de Cristo Mountains, New Mexico (Figure Figs. 1 & 3). The outcrop exposure consists of the crystalline rocks of the Yavapai province, highly deformed compositionally layered quartzofeldspathic gneiss, amphibolitic gneiss, felsite, biotite schist, and granitic pegmatite (Lemen et al., 2015), overlain by the Devonian to Mississippian shallow marine transgressive sequence of carbonate and ealstieclastic rocks of the Espiritu Santo Formation. The Espiritu Santo Formation consists of primarily limestone and dolomitic limestone, with a basal conglomeratic sandstone known as the Del Padre Member (Baltz and Myers, 1999). The Espiritu Santo Formation consists of primarily limestone and dolomitic limestone, with a basal conglomeratic sandstone known as the Del Padre Member (Baltz and Myers, 1999). The rocks are exposed within the Sangre de Cristo Mountains, north-trending fault bounded blocks uplifted during the Neogene Laramide Orogeny (Baltz and Myers, 1999; Lessard and Bejnar, 1976). This site location provides an analogue for the Raton Basin to the east where injection in Class II wells has been linked to basement earthquakes since 2001 (Nakai et al., 2017; Rubinstein et al., 2014).

### 2.1.2 Core samples

The R.C. Taylor 1 core samples the Cambrian LamotteLa Motte Formation sandstone and sheared Proterozoic granitoids in the Central Plains Orogen of the 1.6 Ga Yavapai-Mazatal Province (Marshak et al., 2017; Sims, 1990; Whitmeyer and Karlstrom, 2007) (Fig 1). The borehole was drilled adjacent to the Cambridge Arch and is associated with a series of northwest trending transpressional faults of the Central Plains orogeny Orogen (Sims, 1990; Whitmeyer and Karlstrom, 2007) (Whitmeyer and Karlstrom, 2007; Sims, 1990) (Figure X Fig. 4). In this core, the arkosic LamotteLa Motte Formation, regionally called the

Formatted: Heading 2, Adjust space between Latin and Asian text, Adjust space between Asian text and numbers

Formatted: Font: (Default) Times New Roman

Formatted

Formatted: Font: (Default) Times New Roman, 10 pt, Eng (United Kingdom)

Formatted: Line spacing: 1.5 lines

Formatted

Formatted

Field Code Changed

Field Code Changed

Formatted

125 Reagan and Sawatch Sandstones, is a fine-grained, well-sorted glauconitic sandstone deposited during a transgression and is  
an analogue for Cambrian sandstones being evaluated for deep injection and storage of CO<sub>2</sub> (Carr et al., 2005; Miller, 2012).  
130 The CPC BD-139 core, recovered from the Michigan Basin samples the contact between the Cambrian Mount Simon  
Sandstone and Precambrian altered granitoid gneiss of the Grenville Front Tectonic Zone (Figure XFig. 1 & 5). The  
Precambrian gneiss-crystalline rocks captured in this core is-are characterized as granitic to tonalitic gneissgneiss of Easton  
and Carter, 1995) that form the basement of the Michigan Basin. The Michigan Basin is a thermally complex intracratonic  
basin situated over the lower peninsula of Michigan. Unexpectedly high levels of thermal maturity in the Paleozoic strata of  
the basin is thought to be attributed to elevated basal heat flow occurring up until Silurian time, as well as the prior existence  
of ~2 km of Pennsylvanian and Permian strata that has since been eroded (Everham and Huntoon, 1999). The Mount Simon  
Sandstone reservoir is a unit of deep wastewater injection in Oklahoma and it is also targeted for CO<sub>2</sub> storage (Barnes et al.,  
135 2009; Dewers et al., 2014; Leetaru et al., 2009; Liu et al., 2011).

The BO-1 core samples the lower Cambrian Mount Simon Sandstone overlying a Precambrian layered intrusive complex of  
altered and altered gabbro, other mafic intrusions and felsic dikes (Smith et al., 2019; Fig. 406). The crystalline basement  
rocks are part of the Northeast Iowa Intrusive Complex and are hypothesized to be a part of the Midcontinent Rift System  
140 (Anderson, 2012). The Midcontinent Rift System extends from Kansas to Lake Superior and then southward through  
Michigan (Figure Fig. 1). The geologic features associated with the Midcontinent Rift System, include axial basins filled  
with basalt and immature clastic rocks along with evidence of crustal extension(Ojakangas et al., 2001) . The BO-1 core is  
analogous to several geologic settings anticipated in the subsurface of midcontinent region where lower Cambrian to upper  
Ordovician rocks directly overly Precambrian mafic igneous rocks of the Midcontinental Rift System along the Great  
145 Unconformity (Gilbert, 1962; Mossler, 1995). Northwest trending fault systems near the borehole were identified by  
magnetic lineaments and are likely part of the regional NW-SE Belle Plaine Fault Zone (Drenth et al., 2015). The  
Midcontinent Rift System is being studied for deep injection of CO<sub>2</sub> (Abousif, 2015; Wickstrom et al., 2010).

### 3 Characterization of the nonconformity

Given the recognized importance of direct fluid transmission, variation in pressure, and poroelastic loads on induced seismicity  
150 (Chang and Segall, 2016; Ortiz et al., 2019; Yehya et al., 2018; Zhang et al., 2013), we provide an overview of rock properties  
observed at the nonconformity using integrated outcrop-based studies in Michigan and New Mexico, and analyses of core from  
Michigan, Minnesota and Nebraska (Fig. 1).

#### 3.1 Methods

To describe the nonconformity zone in core and outcrop and document structures and mineralogy across the boundary, we  
155 use a variety of micro- to meso-scale methods including lithological and structural logging of outcrop and core, optical thin-

Formatted: Subscript, Not Highlight

Formatted: Not Highlight

Formatted: Font: 10 pt

Formatted: Font: 10 pt

Formatted: Highlight

Formatted: Font: 10 pt

Formatted: Font: 10 pt

Formatted: Font: 10 pt

Formatted: Font: 10 pt

Formatted: Font: 10 pt

Formatted: Font: 10 pt

Formatted: Font: (Default) Times New Roman, 10 pt, Font color: Black

Formatted: Font: (Default) Times New Roman, 10 pt, Font color: Black, Not Superscript/ Subscript

Formatted: Font: (Default) Times New Roman, 10 pt, Font color: Black

Formatted: Font: 10 pt

Formatted: Font: (Default) Times New Roman

Formatted: Default, Line spacing: 1.5 lines

Formatted: Font: 10 pt

Formatted: Default, Space Before: 0 pt, Line spacing: 1. lines

Formatted: Font: 10 pt

Formatted: Font: 10 pt

Formatted: Font: 10 pt

Formatted: Font:

Field Code Changed



section petrography and x-ray diffraction (XRD) mineralogic studies, whole-rock x-ray fluorescence (XRF) elemental analysis, and gas or air permeability measurements, when possible. We evaluated fracture distribution in outcrop and core noting fracture type, vein, fault, or joint and associated mineralogy. XRD and XRF was carried out at Utah State University (USU) X-ray analysis laboratory and XRD was carried out at Western Colorado University (WCU) petrography laboratory. At USU XRD analyses were done using a Panalytical X'Pert Pro X-ray Diffraction Spectrometer (40 mA and 45 kV) with monochromatic CuK $\alpha$  radiation utilizing X'Pert Highscore software for phase analysis. XRF analyses were performed using a portable Bruker Energy Dispersive X-ray Fluorescence Spectrometer utilizing S1PXRF, Microsoft Excel, and ARTAX software packages for elemental analysis. At WCU XRD analysis was done using a Bruker D8 X-ray Diffraction Spectrometer (40 mA and 45 kV) with monochromatic CuK $\alpha$  radiation utilizing DIFFRAC.SUITE software for phase analysis.

Twenty-five samples from BO-1 drillcore were selected for gas permeability testing through Schlumberger Rock Mechanics and Core Analysis Services. Profile permeability measurements were made in steady state conditions with a mini permeameter where gas is injected directly onto the core slab surface. The profile permeameter has a measurable permeability range of 0.1 millidarcies to 3 darcies.

To illustrate effects of a reduced permeability above the nonconformity on fluid migration we compare three hydrogeologic models of basal reservoir injection that consider continuous and discontinuous zones of altered low permeability rocks above the basement (Fig. 13). Each model run includes a 100 m-thick basal reservoir ( $3 \times 10^{-15} \text{ m}^2$ ) underlain by 9.9 km of relatively low permeability ( $k_x = k_z = 3 \times 10^{-17} \text{ m}^2$ ) crystalline basement rock. A 20 m-wide conduit-barrier fault ( $k_x/k_z=105$ ;  $k_z = 3 \times 10^{-10} \text{ m}^2$ ) is present in all simulations as is an injection well located 150 m from the fault zone. Wellhead pressures reached over 50 m excess hydraulic head after 4 days in response to 5000 m<sup>3</sup>/day of continuous injection.

## 2.3.2 Results

### 2.3.2.1 Lake Superior, Michigan

Outcrops of the nonconformity between late Proterozoic Jacobsville Sandstone and early Proterozoic altered peridotite crystalline basement are exposed at Presque Isle and Hidden Beach along the southern shore of Lake Superior, Michigan (Lewan, 1972). The Jacobsville Sandstone (Hamblin, 1958) consists of a variably indurated pebble to cobble conglomerate and a lenticular planar to cross-bedded light red quartz arenite (Fig. 2), at Presque Isle the topographic relief of the basement nonconformity varies by 2.5 m over a distance of 1100 m of outcrop (Cuccio, 2017). At these localities the Jacobsville Sandstone (Hamblin, 1958) consists of a variably indurated pebble to cobble conglomerate and a lenticular planar to cross-bedded light red quartz arenite (Fig. 2).

At Presque Isle, a mineralized conglomerate is in direct contact with the underlying serpentinized peridotite or is transitionally interbedded with the overlying sandstone (Fig. 2B). Where present, the low-porosity conglomerate consists of sub-angular to

Formatted: Font: (Default) +Body (Times New Roman), 1 pt, English (United Kingdom)

Formatted: Font: (Default) +Body (Times New Roman), 1 pt, English (United Kingdom)

Formatted: Font: (Default) +Body (Times New Roman), 1 pt, English (United Kingdom)

Formatted: Highlight

Formatted: Left, Pattern: Clear (White)

Formatted: Normal, Don't adjust space between Latin and Asian text, Don't adjust space between Asian text and numbers

Field Code Changed

rounded chalcedony, gneiss, and greenstone cobble clasts with fine-grained, poorly sorted, hematite cemented angular quartz grains.

At Hidden Beach, poorly consolidated basal conglomerates of the Jacobsville Sandstone are in contact with the Precambrian Compeau Creek Gneiss. The quartz arenite consists of fine-grained, angular, moderately sorted quartz with some feldspar.

Distinctive bleached fractures or reduction spots are associated with the lower Jacobsville Sandstone and range in orientation from near-vertical to bedding-parallel. ~~bleached fractures or reduction spots are associated with the lower Jacobsville Sandstone and~~ The near-vertical reduction fractures (Fig. 2C) are not observed to extend into the basement (Fig. 2C). ~~basement.~~ Locally, basement-hosted slip surfaces are coated with epidote-iron oxide and are sub-parallel to the ~~roughly align with the near-vertical bleached fractures~~ zones in the overlying Jacobsville Sandstone (Fig. 2C).

Optical petrography across the transition from red sandstone protolith to a bleached fracture zone at Hidden Beach reveals a reduction in hematite grain coatings and cements. Whole-rock XRF analysis of the bleached areas of Jacobsville Sandstone indicates a minor depletion of K<sub>2</sub>O, and a minor enrichment of FeO and MgO, relative to the unaltered Jacobsville Sandstone (Figure Fig. 37). At Presque Isle, mineral alteration products in the conglomerate include nontronite, with trace zeolites and iron oxides (Fig. 37). The underlying serpentized peridotite is black to brown, with abundant white carbonate mesh veinlets and localized stockwork jasperoid veins up to 10 cm wide. ~~Jasperoid mineralization occurs along a few small faults that span the contact.~~ cross the nonconformity (Cuccio, 2017).

### 23.2.2 Gallinas Canyon, New Mexico

Devonian to Mississippian carbonate and clastic rocks of the Espiritu Santo Formation deposited on the Proterozoic quartzofeldspathic and amphibolitic gneiss, biotite schist, and granitic pegmatite (Lemen et al., 2015) are exposed along a 4-km long section in Gallinas Canyon, eastern Sangre de Cristo Mountains, New Mexico. The nonconformity is cut by cm- to m's - displacement faults, where at this location we characterize both the faulted and the adjacent-un-faulted nonconformity zone (Hesseltine, 2019; Kerner, 2015). Top of basement is defined by phyllosilicate rich zone with variable thickness, 0 to >5 m, that is truncated by the Del Padre Sandstone. Locally the Del Padre Sandstone is laterally discontinuous (Hesseltine, 2019) but is reported to be up to 15 m thick filling depressions in underlying crystalline rock elsewhere in New Mexico (Armstrong & Mamet, 1974). The carbonate and clastic rocks of the Espiritu Santo Formation include: 1-m thick massive, fine-grained, rounded to sub-rounded sandstone with calcite nodules, ~1- m of microcrystalline dolomite that transitions upward into a chert nodule limestone, interbedded mudstone and limestone and a massive microcrystalline limestone bed. A phyllosilicate-rich zone directly below the nonconformity is approximately 60-cm thick and is a poorly lithified zone that marks the transition from highly altered (weathering and hydrothermal alteration) to minimally altered crystalline rock (Fig. 48). The Precambrian crystalline rocks are cut by large thrust faults and smaller scale normal faults (Baltz and Myers, 1999; Lessard and Bejnar, 1976) with some juxtaposing sedimentary and crystalline rock (Fig. 3D). In the Gallinas Canyon, the crystalline rock is overlain by the 0.5 to 1.5 m thick marine Del Padre Sandstone, silica and calcite-cemented, grayish-olive and tan, jointed, fine to very coarse-grained sandstone (Baltz and Myers, 1999).

Formatted: Font:

Field Code Changed

Formatted: Font:

Field Code Changed

Formatted: Font:

Field Code Changed

Formatted: Highlight

Formatted: Highlight

Formatted: Font: (Default) +Body (Times New Roman)

Formatted: Highlight

Formatted: Highlight

Formatted: Highlight

Formatted: Font: (Default) +Body (Times New Roman)

Formatted: Highlight

220 The predominant lithology of the crystalline basement is gneiss, with minor schist, pegmatitic granite, and basalt. Mineral alteration is greatest directly below the nonconformity. This zone is enriched in sericite within feldspars, and clay minerals (mixed with hematite and associated with replacement of micas) (Fig. 58). Where cut by faults the nonconformity-associated phyllosilicates form a matrix that surrounds more rigid grains such as quartz, suggesting deformation in this unit was accommodated by granular flow, a process associated with high pore-fluid pressure (Paterson, 2012). Microscopic fracturing has occurred within the crystalline basement, these fractures are mineralized with iron oxide, sericite, chert, and calcite. The majority of fractures within the crystalline basement occur along weak grains such as sericitized feldspar and altered mica or cut across quartz and feldspar grains. Authigenic calcite is rare within the crystalline basement, though commonly occurs as coarsely crystalline calcite cement within grain fractures in feldspar and sericitized feldspar.

230 ~~Fractures-Where faults cut the altered crystalline basement locally and cataclasites are found throughout the fault core in crystalline basement but are absent within protolith crystalline basement.~~ Where faulted, the sedimentary rock damage zone includes large twinned calcite grains in fracture-filling cements, and cataclasites that lie along the edges of the calcite veins. These cataclasites include: pulverized quartz and feldspar grains, chert, pulverized protolith, as well as clay- and iron oxide-rich minerals. Quantitative microprobe analyses of the carbonate and fine-grained matrix composition within the sedimentary and basement fault cores reveals that all calcite vein elemental values have a slightly reduced level of ~~iron-Fe~~ and Mg substitution for Ca than the calcite matrix. The fine-grained matrix within the sedimentary fault core is nearly pure silica, whereas the fine-grained matrix within the crystalline basement fault core is aluminium-rich (Fig. 58).

### 23.2.3 R.C. Taylor 1 Core, Nebraska

Core from the R.C. Taylor 1 wildcat well was obtained in 1953 in south-central Nebraska. We examined a total of 19.2 m of core recovered over the Cambrian LamotteLa Motte Formation sandstone and sheared Proterozoic granitoids in the Central Plains Orogen of the Yavapai Province (Marshak et al., 2017; Sims, 1990; Whitmeyer and Karlstrom, 2007). The arkosic LamotteLa Motte Formation, regionally called the Reagan and Sawatch Sandstones, is a fine-grained, well-sorted glauconitic sandstone (Fig. 6).

The basal LamotteLa Motte Formation is cut by quartz, calcite, dolomite, and iron-oxide veinlets (Fig. 78). Iron-oxide veins cut quartz veins, and both are cut by calcite veins, providing evidence for three mineralization events here (Fig. 79). Below the LamotteLa Motte Formation is a phyllosilicate-rich zone composed of 40 cm thick highly altered basement shear zone that overlies a minimally altered basement shear zone, both are comprised of fine crystalline sericitized feldspar and chlorite-rich shear zones, and overlie the coarse-crystalline, minimally altered granitic basement containing some sericitized feldspar (Fig. 79).

245 The altered basement shear zone is composed of quartz, feldspar, biotite, chlorite, and dolomite (Fig. 79). Quartz and feldspars are disintegrated, well-developed chlorite, hematite and magnetite are altered from biotite, and granular disintegration has resulted in clay development. Open pore-space occurs between host-rock grains and neofomed clays. The basement shear zone is characterized by feldspar, quartz, mica, and the alteration minerals chlorite and dolomite (Fig. 79). The shear zones

Field Code Changed

Formatted: Highlight

contain ~~chlorite lined fractures~~, slip surfaces, and S-C fabrics within chloritized zones. The shear fabrics are cut by quartz, sparry calcite, iron-oxide and dolomite veins. The basal, moderately altered basement unit is a coarse-crystalline granite composed of feldspar, quartz, biotite, and hornblende (Fig. 79). Chlorite is present and associated with minor shear fabrics. Calcite, dolomite, and quartz veins parallel and cross-cut the chlorite-rich shear fabrics and cut quartz and feldspar crystals (Fig. 79). In the coarse-crystalline granite altered feldspars contain sericite that has formed adjacent to twin planes. Veins of dolomite, calcite, and hematite occur in the lower 7 m of the ~~Lamotte~~La Motte Formation and are observed through the underlying granitic shear zone covering 12.5 m of core.

#### 23.2.4 CPC BD-139 Core, Michigan

The CPC BD-139 core, obtained in 1964 for the design of a brine disposal well, samples the contact between the Cambrian ~~Mt. Simon~~Mount Simon Sandstone and Precambrian altered granitoid gneiss of the Grenville Front Tectonic Zone. We divide the CPC DB-139 core into three lithologic units: a laminated sandstone, a finely foliated gneiss, and a gneiss with sub-horizontal white veins. Both gneiss units have zones of dolomitization. ~~The Mount Simon Sandstone reservoir is a unit of deep wastewater injection in Oklahoma and it is also targeted for CO<sub>2</sub> storage (Dewers et al., 2014).~~ Measured porosity values of the Mount Simon Sandstone range from 11-18% (Wisconsin Geological Natural History Survey, 2019).

Sandstone grains are rounded to sub-rounded and moderately to well-sorted. A discrete boundary separates the ~~Mt. Simon~~Mount Simon Sandstone from the underlying altered granitoid gneiss (Fig. 810). The uppermost 30 cm of the basement is composed of tan, fine-grained, dolomite horizon which grades into a dark green foliated gneiss cut by pink sub-vertical fractures over a span of ~5 cm (Fig. 810). The basal meter of the ~~Mt. Simon~~Mount Simon Sandstone is a tan, finely laminated arenite with minor amounts of iron-rich clay. The quartzo-feldspathic granitoid gneiss near the contact contains the following alteration products: zeolites, vermiculite, and Fe-, Mn-oxides, and carbonates including dolomite (Fig. 910). Dolomitization of the basement host rock re-appears ~2 meters below the nonconformity. The original basement foliation is preserved and is associated with micrometer-scale crystalline dolomite grains, radiating silica crystals, and sub-horizontal calcite and dolomite veins (Fig. 910). Trace amounts of ankerite, clinocllore, and vermiculite are also present in the dolomitized basement rocks (Fig. 910).

The Cambrian Mt. Simon Sandstone in the Michigan Basin is characterized as a porous (5-15% pore space) arenite to sub-arkosic sandstone (Leeper et al., 2012). Permeability in the basal Mt. Simon Sandstone is reported to be between  $1 \times 10^{-16} \text{ m}^2$  to  $1 \times 10^{-12} \text{ m}^2$  (Frailey et al., 2011).

#### 23.2.4 BO-1 Core, Minnesota

The BO-1 core was originally collected in 1962 as part of an exploratory mining project in Fillmore County, southeast Minnesota (Gilbert, 1962). This core provides a continuous 300 m section of altered and mineralized rocks of lower Cambrian

Field Code Changed

285 Mount Simon Sandstone overlying a Precambrian layered intrusive complex of altered and unaltered gabbro, other mafic intrusions and felsic dikes (Smith et al., 2019; Fig. 4011).

Sedimentary sequences in BO-1 extend to ~ 1.2 km where the nonconformity is marked by an ~ 12 cm zone of pervasive leaching and iron-hydroxide staining (goethite). Intense alteration extends into the basement rocks for ~ 21 m, with ~ 50 m of argillitic and propylitic alteration, ~~multi-layered veins~~, and/or fracture mineralization observed to ~ 402 m depth (Fig. 4011). Localized fault and fracture surfaces intersect the sampled basement core from within ~ 1 cm of the nonconformity contact and extend to 475.5 m, fracture density decreases with depth (Fig 11). Slip surfaces exhibit oblique to dip-slip slickenlines and range from mm's to cm's thick and are either coated in clay or contain mineral infillings ( $\pm$ carbonate,  $\pm$ silica,  $\pm$ chlorite,  $\pm$ iron-oxides).

295 The ~~porous Mt. Simon~~Mount Simon Sandstone contains a ~ ~~0.5-meter~~0.5-meter zone of intense iron-hydroxide (goethite) alteration at the nonconformity (Fig. 4011). This iron-hydroxide oxidized zone extends for several m's into the slightly altered and metamorphosed crystalline basement rock. From petrographic and ~~X-ray diffraction~~XRD analyses, we identify mineralogical assemblages (Fig. 11); dolomite, siderite, iron-oxides, iron-hydroxides, illite, smectite, kaolinite-serpentinite, vermiculite) and textures that are indicative of weathering, diagenesis, and multiple episodes of fluid-rock interactions coupled with deformation within the broad ~ 50 m zone of intense alteration marked by the abundant structural discontinuities across the nonconformity zone (Fig. 11).

300 Measured gas permeability values are highest above the nonconformity within the porous ~~Mt. Simon~~Mount Simon sedimentary reservoir (up to 1000 millidarcy) and vary significantly from 0-500 millidarcy below the nonconformity contact. ~~Locally~~Locally permeability increases in direct correlation to the presence of structural discontinuities (Fig. 406).

### 3.3 Hydrogeologic models

305 The first model (Fig. 43A12A) is a Type 0 nonconformity, represented by a sharp contact between basement and overlying injection reservoir. In the second model simulation, a Type I nonconformity, we included a 20-m-thick, low-permeability ( $k_x=k_z=3\times 10^{-18}$  m<sup>2</sup>) zone (Fig. 43B12B); this layer is 1 order of magnitude less permeable than the basement host rock and a further 1 order of magnitude less permeable in the fault core. The continuous low permeability zone reduces the permeability of the basement fault damage zone by 4 orders of magnitude, making the fault damage zone non-conductive. Pressure does not propagate into the crystalline basement although there was some diffusion of the 2-m excess hydraulic head front to depths  $\leq$  500 m. In the third simulation, a discontinuous low permeability zone is present (Fig. 43C12C). Where this zone is absent, the pressure front propagates into the basement along the fault damage zone to a depth of 2.5 km. The fault zone was not blocked by the low permeability zone, and elevated pore pressures propagated downward to depths of 2.5 km via the fault zone (Fig. 43C12C). Elevated fluid pressures likewise appeared to be forced down other areas where the low permeability zone pinches out, such as towards the right-hand side of Fig. 43C12C.

Field Code Changed

Formatted: Heading 3

Commented [EP1]: Move figure

Formatted: Highlight

Formatted: Highlight

Formatted: NMT\_Thesis\_Body\_Normal, Line spacing: 1.5 lines

### 3.4 Discussion

The nonconformities examined in this study range from sharp contacts to zones several m's thick and exhibit a range of mineralized textures and structural discontinuities (Supplementary Table 1). We observe mineralogic alterations across the nonconformity that are expected to impact diffusivity and storativity, and the sites evaluated provide geological and hydrogeological analogues that aid in understanding the impact circulating fluids may have on altering rock properties at depth (Oliver et al., 2006). Based on observations made in this work, we divide nonconformities into three end-member types, (Table 1), Type 0 – a sharp contact between sedimentary strata and basement rocks; Type I – an interface dominated by phyllosilicates; and Type II – an interface dominated by non-phyllosilicate secondary mineralization. All the nonconformity types observed in this study are cut by structural discontinuities, therefore several possible contact sub-types exist within these 3 proposed end members (Fig. 13). Based on our observations structural and mineralogical heterogeneities at the sedimentary-crystalline rock nonconformity are thought to control the degree to which fluids, fluid pressure, and associated poroelastic stresses are transmitted over long distances across and along the nonconformity boundary. The structural elements and fluid-related alteration patterns observed in these analogue sites support the hypothesis that the nonconformity interface zone influences or controls the potential for cross-contact fluid flow and distribution of fluids within the crust.

Our collective field and core observations in various basement tectonic settings document the occurrence of significant variations in altered or mineralized zones that lead to contrasts in permeability across the nonconformity. Where present the structural discontinuities includes small offset faults, shear fractures, and veins. In thin-section we note evidence for dissolution, recrystallization, new mineral growth, and veins that reflect mineralization or deformation at depth and are not the result of alteration due to weathering alone. Crack-seal textures and calcite twinning lamella, suggest vein mineralization at depth (Burkhard, 1993), and reactivation of pre-existing fractures document episodic fracture growth (Davatzes and Hickman, 2005; Laubach et al., 2004).

At a Type 0 nonconformity, the nonconformity zone is expected to prevent direct fluid pressure communication across the contact due to a significant contrast in rock permeabilities that would hinder cross-contact fluid migration while promoting migration parallel to the contact distributing fluids laterally away from the injection site (Fig. 13A); at a Type I nonconformity, a phyllosilicate dominated contact is expected to inhibit fracture propagation across the nonconformity (Ferrill et al., 2012; Larsen et al., 2010; Schöpfer et al., 2006) and therefore maintain a significant permeability contrast preventing direct fluid migration. In such cases, nonconformities result in a poor hydrologic connection between the sedimentary section and deeper basement rocks (13B).

However, repeated brittle failure and mineralization, observed in Type I nonconformities, suggest that phyllosilicate dominated shear zones can act as a zone of mechanical weakness that can be reactivated allowing for development of fracture permeability. In this fractured nonconformity we observed alteration as deep as 5 m below the nonconformity in the crystalline rocks examined, however, previous work highlights the potential for fractures and connectivity to basement fault zones at

much greater depths (Duffin et al., 1989). Pre-existing basement shear zones that are reactivated may allow future fluid circulation during injection scenarios.

350 Type II nonconformities (Table 1, Fig. 13C, Supplemental Table 1) are mineralized contacts, that include secondary alteration minerals found within 10 cm to several m's below the nonconformity. The mineralization due to fluid-rock interactions at the Type II nonconformities suggests that deep fluid circulation occurs even without enhanced permeability from fractures (Cuccio, 2017) (Fig. 12C). This nonconformity type could prevent brittle deformation but may be more influenced by poroelastic loads. The impact of these contacts on hydrogeologic properties is not yet well understood or modelled.

355 The impact the morphology of the nonconformity has on the downward propagation of fluid pressures into the crystalline basement has been shown by several numerical hydrogeologic studies (Ortiz et al., 2019; Segall and Lu, 2015; Yehya et al., 2018; Zhang et al., 2016). These models suggest that direct pore-fluid pressure communication (Ortiz et al., 2019; Segall and Lu, 2015; Yehya et al., 2018) and significant changes in poroelastic stress (Goebel and Brodsky, 2018; Zhang et al., 2016) can occur well way from the injection zones. Numerical models predict that nonconformities with through-going fractures distribute fluid deeper into the basement rocks and that direct pore pressure communication can destabilize faults at depth (Ortiz et al., 2019; Segall and Lu, 2015; Yehya et al., 2018). All the nonconformity types observed here are cut by structural discontinuities, and several possible contact sub-types exist within these 3 proposed end member scenarios (Fig. 12). Fractures, and especially fault zones, are expected to distribute fluids and propagate fluid pressures to a greater depth regardless of nonconformity type (Yehya et al., 2018). Because nonconformity interface zones with pre-existing deformation fabrics may be preferential flow pathways that distribute fluid pressure away from the injection zone, high-permeability damage zones transmit fluid pressure to greater depths than non-conduit fault zones (Yehya et al., 2018).

360 To illustrate effects of a reduced permeability above the nonconformity and the impact of permeable fault zones on fluid migration we compare three models of basal reservoir injection that consider continuous and discontinuous zones of altered low permeability rocks above the basement (Fig. 12). The Type 0 nonconformity, represented by a sharp contact between basement and overlying injection reservoir, results in lateral migration away from the injection well and downward migration where it encounters a fault zone (12A). In the second model simulation, a Type I nonconformity, the presence of a 20-m-thick, low-permeability zone and no connection between basement and sedimentary fault zones results in lateral migration and pressure does not propagate into the crystalline basement (Fig. 12B). In the third simulation, models a Type I nonconformity with a discontinuous low permeability zone, where this zone is absent, the pressure front propagates into the basement along the connected fault damage zone to a depth of 2.5 km and elevated fluid pressures appear to be forced downward were the low permeability zone pinches out (Fig. 13C).

370 Our collective field and core observations document the occurrence of significant variations in altered or mineralized zones which would impact permeability values associated with the nonconformity zone, and that alteration coupled with abundant structural discontinuities can result in relatively higher permeability that extends for 10's of meter's both into the crystalline basement rock below the nonconformity.

380

Formatted: Font: (Default) +Body (Times New Roman)

Formatted: Normal, Line spacing: single, Tab stops: 0.1 Left

#### 4.5 Conclusions

We define key rock types and structural elements of the nonconformity zone and split the analogue nonconformities into three end-member types. The three non-conformity end member types provide a broad hierarchy of nonconformities in the midcontinent (Supplemental Table 1) and are observed at nonconformity sites elsewhere. The geologic conditions associated with the nonconformities documented here can be used to help constrain the permeability architecture that impacts both diffusivity and storativity at and across the nonconformity. We expect these nonconformity types to either distribute fluid pressure away from the injection point or provide direct communication with basement rocks, distributing fluids to a greater depth across the nonconformity. We observe that fractures cut all nonconformity types and expect in these cases that changes in fluid pressure or poroelastic loads could result in triggered earthquakes within basement rocks (Chang and Segall, 2016; Zhang et al., 2013). Numerical modelling of Type 0 and Type I end members that include fault zones predict downward propagation of fluid pressure and changes to poroelastic loads. The data presented here can be used to improve model inputs for evaluation of cross-contact fluid and pressure communication whether through creation or modification of existing permeability or poroelastic pathways or through rheological changes associated with fluid-rock interactions. We show that *in-situ* conditions along the nonconformity zone vary, and observe common, localized, high permeability zones. The data from outcrop and core observations also suggest that injection of brines at depth may drive mineralogical alteration and potential fault zone weakening, these data can also be used to understand the impact that long-term storage of chemically reactive fluids has on rock properties. Our observations illustrate that the contact should not be treated as an impermeable barrier to fluid flow nor as one cut by faults of various permeabilities but should instead be evaluated on a site by site basis prior to injection of large fluid volumes.

Formatted: Not Highlight

Field Code Changed

#### 5.6 Acknowledgements

This work was supported by collaborative NEHRP grants #G15AP00080 and #G15AP00081 awarded to Evans, Bradbury, Person, and Mozley, a Western State Colorado University Professional Activity Fund grant to Petrie, and a USGS-USU cooperative agreement #G17AC00345 to Bradbury and Evans. Additional student support obtained from student research grants from the Geological Society of America (GSA) awarded to Cuccio, Hesselstine, and Smith, the GSA Stephen E. Laubach Structural Diagenesis Award to Smith, and a GDL Foundation grant to Cuccio.



## References

- 410 [Abousif, A. M. A.: Mineral and geochemical attributes of the midcontinent rift sequence; An application for deep carbon dioxide sequestration, 2015.](#)
- [Anderson, R.: U.S. Geological Survey Airborne Study of Northeast Iowa, Iowa Geological & Water Survey., 2012.](#)
- [Armstrong, D. K. and Carter, T. R.: The subsurface Paleozoic stratigraphy of Southern Ontario, Ontario Geological Survey, Sudbury, Ontario., 2010.](#)
- 415 [Baltz, E. H. and Myers, D. A.: Stratigraphic framework of upper Paleozoic rocks, southeastern Sangre de Cristo Mountains, New Mexico, with a section on speculations and implications for regional interpretation of Ancestral Rocky Mountains paleotectonics., New Mexico, Bureau of Mines and Mineral Resources, Socorro, New Mexico, USA., 1999.](#)
- 420 [Barnes, D. A., Bacon, D. H. and Kelley, S. R.: Geological sequestration of carbon dioxide in the Cambrian Mount Simon Sandstone: Regional storage capacity, site characterization, and large-scale injection feasibility, Michigan Basin, Environmental Geosciences, 16\(3\), 163–183, 2009.](#)
- [Carr, T. R., Merriam, D. F. and Bartley, J. D.: Use of relational databases to evaluate regional petroleum accumulation, groundwater flow, and CO2 sequestration in Kansas, AAPG bulletin, 89\(12\), 1607–1627, 2005.](#)
- 425 [Chang, K. and Segall, P.: Injection-induced seismicity on basement faults including poroelastic stressing, Journal of Geophysical Research: Solid Earth, 121\(4\), 2708–2726, 2016.](#)
- [Cuccio, L.: Geological Characterization of Precambrian Nonconformities: Implications for Injection-Induced Seismicity in the Midcontinent United States, Utah State University., 2017.](#)
- 430 [Dewers, T., Newell, P., Broome, S., Heath, J. and Bauer, S.: Geomechanical behavior of Cambrian Mount Simon Sandstone reservoir lithofacies, Iowa Shelf, USA, International Journal of Greenhouse Gas Control, 21, 33–48, doi:10.1016/j.ijggc.2013.11.010, 2014.](#)
- [Drenth, B. J., Anderson, R. R., Schulz, K. J., Feinberg, J. M., Chandler, V. W. and Cannon, W. F.: lies beneath: geophysical mapping of a concealed Precambrian intrusive complex along the Iowa–Minnesota border, Canadian Journal of Earth Sciences, 52, 279–293, doi:10.1139/cjes-2014-0178, 2015.](#)
- 435 [Duffin, M. E., Lee, M., Klein, G. D. and Hay, R. L.: Potassic diagenesis of Cambrian sandstones and Precambrian granitic basement in UPH-3 deep hole, Upper Mississippi Valley, USA, Journal of Sedimentary Research, 59\(5\), 1989.](#)
- [Easton, R. M. and Carter, T. R.: Geology of the Precambrian basement beneath the Paleozoic of southwestern Ontario, in Basement Tectonics 10, pp. 221–264, Springer., 1995.](#)

**Formatted:** Bibliography, Widow/Orphan control, Adjust space between Latin and Asian text, Adjust space between Asian text and numbers

**Field Code Changed**

- 440 Ellis, M. A., Laubach, S. E., Eichubul, P., Olson, J. E. and Hargrove, P.: Fracture development and diagenesis of Torridon Group Applecross Formation, near AnTeallach, NW Scotland: millennia of brittle deformation resilience?, Journal of the Geological Society, 169, 297–310, 2012.
- 445 Ellsworth, W. L., Llenos, A. L., McGarr, A. F., Michael, A. J., Rubinstein, J. L., Mueller, C. S., Petersen, M. D. and Calais, E.: Increasing seismicity in the U. S. midcontinent; implications for earthquake hazard (in Injection-induced seismicity), The Leading Edge, 34(6), 618–626, 2015.
- Everham, W. D. and Huntoon, J. E.: Thermal history of a deep well in the Michigan Basin: Implications for a complex burial history, in Geothermics in Basin Analysis, pp. 177–202, Springer., 1999.
- Gair, J. E. and Thaden, R. E.: Geology of the Marquette and Sands Quadrangles, Marquette County, Michigan., 1968.
- 450 Gilbert, R. C.: Final Report Minnesota Project (Area 4) Fillmore County, Minnesota, The New Jersey Zinc Company, Platteville Wisconsin., 1962.
- Goebel, T. H. W. and Brodsky, E. E.: The spatial footprint of injection wells in a global compilation of induced earthquake sequences, Science, 361, 899–904, 2018.
- Hamblin, W. K.: The Cambrian sandstones of northern Michigan, University of Michigan., 1958.
- 455 Hesseltine, G.: Micro- To Macro-Scale Structural And Lithological Architecture Of Basal Nonconformities: Implications For Fluid Flow And Injection Induced Seismicity, MS, Utah State University, Logan, UT., 2019.
- Hoffman, P.: United Plates of America the birth of a craton: Early Proterozoic assembly and growth of Laurentia, Annual Review of Earth and Planetary Sciences, 16, 543–603, 1988.
- 460 Karlstrom, K. E. and Humphreys, E. D.: Persistent influence of Proterozoic accretionary boundaries in the tectonic evolution of southwestern North America: Interaction of cratonic grain and mantle modification events, Rocky Mountain Geology, 33(2), 161–179, 1998.
- 465 Keranen, K. M., H.M, S., G.A, A. and Cochran, E. S.: Potentially induced earthquakes in Oklahoma, USA: Links between wastewater injection and the 2011 Mw 5.7 earthquake sequence, Geology, 41(6), 699–702, 2013.
- Keranen, K. M., Weingarten, M., Abers, G. A., Bekins, B. A. and Ge, S.: Sharp increase in central Oklahoma seismicity since 2008 induced by massive wastewater injection, Science, 25, 448–451, 2014.
- Kerner, K. R.: Permeability architecture of faulted nonconformities: Implications for induced seismicity, New Mexico Institute of Mining and Technology., 2015.

- 470 [Leetaru, H. E. and McBride, J. H.: Reservoir uncertainty, Precambrian topography, and carbon sequestration in the Mt. Simon Sandstone, Illinois Basin, Environmental Geosciences, 16\(4\), 235–243, 2009.](#)
- [Leetaru, H. E., Frailey, S., Morse, D., Finley, R. J., Rupp, J. A., Drahozval, J. A. and McBride, J. H.: Carbon sequestration in the Mt. Simon Sandstone saline reservoir, 2009.](#)
- 475 [Lemen, D., Lindline, J. and Bosbyshell, H.: The Gallinas Canyon gneiss: a window into the nature and timing of Paleoproterozoic events in Northern New Mexico, Geology of the Las Vegas Region., 2015.](#)
- [Lessard, R. H. and Bejnar, W.: Geology of the Las Vegas area, edited by R. C. Ewing and B. S. Kues, New Mexico Geological Society, Inc., Socorro, New Mexico, USA., 1976.](#)
- 480 [Lewan, M. D.: Metasomatism and weathering of the Presque Isle serpentinitized peridotite, Marquette, Michigan \[MS thesis\], 1972.](#)
- [Liu, F., Lu, P., Zhu, C. and Xiao, Y.: Coupled reactive flow and transport modeling of CO<sub>2</sub> sequestration in the Mt. Simon sandstone formation, Midwest USA, International Journal of Greenhouse Gas Control, 5\(2\), 294–307, 2011.](#)
- 485 [Malone, D. H., Stein, C. A., Craddock, J. P., Kley, J., Stein, S. and Malone, J. E.: Maximum depositional age of the Neoproterozoic Jacobsville Sandstone, Michigan: Implications for the evolution of the Midcontinent Rift, Geosphere, 12\(4\), 1271–1282, doi:10.1130/GES01302.1, 2016.](#)
- [Marshak, S., Domrois, S., Abert, C., Larson, T., Pavlis, G., Hamburger, M., Yang, X., Gilbert, H. and Chen, C.: The basement revealed: Tectonic insight from a digital elevation model of the Great Unconformity, USA cratonic platform, Geology, 45\(5\), 391–394, doi:10.1130/G38875.1, 2017.](#)
- 490 [Miller, T. J.: Evaluation of the Reagan and Lamotte Sandstones in Southwestern Missouri for carbon dioxide sequestration, 2012.](#)
- [Mossler, J. H.: Geologic Atlas of Fillmore County, Minnesota, University of Minnesota., 1995.](#)
- [Murray, W. E.: Class II Saltwater Disposal for 2009–2014 at the Annual-, State-, and County- Scales by Geologic Zones of Completion, Oklahoma, Oklahoma Geological Survey, Oklahoma., 2015.](#)
- 495 [Nakai, J. S., Weingarte, M., Sheehan, A. F., Bilek, S. L. and Ge, S.: A possible causative mechanism of Raton Basin, New Mexico and Colorado earthquakes using recent seismicity patterns and pore pressure modeling, Journal of Geophysical Research: Solid Earth, 122, 8051–8065, doi:10.1002/2017JB014415, 2017.](#)
- [Nicholson, C. and Wesson, R. L.: United States Geological Survey, Alexandria, VA., 1990.](#)

- 500 Ojakangas, R. W., Morey, G. B. and Green, J. C.: The Mesoproterozoic Midcontinent Rift System, Lake Superior Region, USA, *Sedimentary Geology*, 141–142, 421–442, 2001.
- Oliver, N. H. S., McLellan, J. G., Hobbs, B. E., Cleverly, J. S., Ord, A. and Feltrin, L.: Numerical models of extensional deformation, heat transfer, and fluid flow across basement-cover interfaces during basin-related mineralization, *Economic Geology*, 101(1), 1–31, 2006.
- 505 Ortiz, J. P.: The role of fault-zone architectural elements and basal altered zones on downward pore pressure propagation and induced seismicity in the crystalline basement, New Mexico Institute of Mining and Technology, Socorro, New Mexico, USA., 2017.
- Ortiz, J. P., Person, M. A., Mozley, P. S., Evans, J. P. and Bilek, S. L.: The role of fault-zone architectural elements on pore pressure propagation and induced seismicity, *Groundwater*, 57, 465–478, doi:10.1111/gwat.12818, 2019.
- 510 Paterson, M. S.: *Materials science for structural geology*, Springer Science & Business Media., 2012.
- Petersen, M. D., Mueller, C. S., Moschetti, M. P., Hoover, S. M., Llenos, A. L., Ellsworth, W. L., Michael, A. J., Rubinstein, J. L., McGarr, A. F. and Rukstales, K. S.: 2016 One-year seismic hazard forecast for the Central and Eastern United States from induced and natural earthquakes., 2016.
- 515 Plains CO2 Reduction (PCOR) Partnership: Plains CO2 Reduction (PCOR) Partnership, CO2 Sequestration Projects in Our Region [online] Available from: <https://undeerc.org/pcor/co2sequestrationprojects/pdf/Print-Friendly-CO2-Sequestration-Projects.pdf>, 2020.
- Rivers, T.: Lithotectonic elements of the Grenville Province: review and tectonic implications, *Precambrian Research*, 86, 117–1545, 1997.
- 520 Rojstaczer, S. A. I. S. E. H. D. O.: Permeability of continental crust influenced by internal and external forcing, *Geofluids*, 8(2), 128–139, 2008.
- Rubinstein, J. L., Ellsworth, W. L., McGarr, A. and Benz, H. M.: The 2001-present induced earthquake sequence in the Raton Basin of northern New Mexico and southern Colorado, *Bulletin of the Seismological Society of America*, 104, 2162–2181, doi:10.1785/0120140009, 2014.
- 525 Segall, P. and Lu, S.: Injection-induced seismicity: Poroelastic and earthquake nucleation effects, *Journal of Geophysical Research*, 120, 5280–5103, 2015.
- Sims, P. K.: *Precambrian Basement Map of the Northern Midcontinent, U.S.A.*, 1990.
- Sims, P. K. and Peterman, Z. E.: Early Proterozoic Central Plains orogen a major buried structure in the north-central United States, *Geology*, 14, 488–491, 1986.
- 530

Sloss, L. L.: Sequences in the cratonic interior of North America., 1963.

Sloss, L. L.: Forty years of sequence stratigraphy. Geological Society of America Bulletin, 100(11), 1661–1665, 1988.

535 Smith, K., Paulding, A., Bradbury, K., Potter, K., Evans, J. and Petrie, E.: Geologic Characterization of the Great Unconformity Injection Interface Region from Field and Drillcore Analog Studies: Implications for Midcontinent Induced Seismicity, Phoenix, AZ, USA., 2019.

Thorleifson, H., Ed.: Potential Capacity for Geologic Carbon Sequestration in the Midcontinent Rift System in Minnesota. [online] Available from: [https://files.dnr.state.mn.us/aboutdnr/reports/MGS\\_CO2\\_Report.pdf](https://files.dnr.state.mn.us/aboutdnr/reports/MGS_CO2_Report.pdf) (Accessed 13 June 2020), 2008.

540 Weingarten, M., Ge, S., Godt, J. W., Bekins, B. A. and Rubinstein, J. L.: High-rate injection is associated with the increase in U.S. mid-continent seismicity. Science, 248(6241), 1336–1340, 2015.

Whitmeyer, S. J. and Karlstrom, K. E.: Tectonic model for the Proterozoic growth of North America. Geosphere, 3(4), 220–259, 2007.

545 Wickstrom, L. H., Venteris, E. R., Harper, J. A., McDonald, J., Slucher, E. R., Carter, K. M., Greb, S. F., Wells, J. G., Harrison III, W. B., Nuttall, B. C., Riley, R. A., Drahovzal, J. A., Rupp, J. A., Avary, K. L., Lanham, S., Barnes, D. A., Gupta, N., Baranoski, M. A., Radhakrishnan, P., Solis, M. P., Baum, G. R., Hohn, M. E., Parris, M. P., McCoy, K., Grammer, G. M., Pool, S., Luckhardt, C. and Kish, P.: Characterization of Geologic Sequestration Opportunities in the MRCSP Region. [online] Available from: [https://www.researchgate.net/profile/Larry\\_Wickstrom/publication/292983481\\_Characterization\\_of\\_Geologic\\_Sequestration\\_Opportunities\\_in\\_the\\_MRCSP\\_Region/links/56b3b4f008ae636a540d1bfb/Characterization-of-Geologic-Sequestration-Opportunities-in-the-MRCSP-Region.pdf](https://www.researchgate.net/profile/Larry_Wickstrom/publication/292983481_Characterization_of_Geologic_Sequestration_Opportunities_in_the_MRCSP_Region/links/56b3b4f008ae636a540d1bfb/Characterization-of-Geologic-Sequestration-Opportunities-in-the-MRCSP-Region.pdf) (Accessed 12 June 2020), 2010.

555 Yehya, A., Yang, Z. and Rice, J. R.: Effect of fault architecture and permeability evolution on response to fluid injection. Journal of Geophysical Research: Solid Earth, 123, 9982–9987, doi:10.1029/2018JB016550, 2018.

560 Zhang, Y., Person, M., Rupp, J., Ellett, K., Celia, M. A., Gable, C., Bowen, B., Evans, J., Bandilla, K., Mozley, P., Dewers, T. and Elliot, T.: Hydrogeologic Controls on Induced Seismicity in Crystalline Basement Rocks Due to Fluid Injection into Basal Reservoirs, Groundwater, doi:10.1111/gwat.12071, 2013.

Zhang, Y., Edel, S. S., Pepin, J., Person, M., Broadhead, R., Ortiz, J. P., Bilek, S. L., Mozley, P. and Evans, J. P.: Exploring the potential linkages between oil-field brine reinjection, crystalline basement permeability, and triggered seismicity for the Dagger Draw Oil field, southeastern New Mexico, USA, using hydrologic modeling. Geofluids, 16(5), 971–987, 2016.

- 565 Anderson, R.: U.S. Geological Survey Airborne Study of Northeast Iowa, Iowa Geological & Water Survey., 2012.  
Armstrong, D. K. and Carter, T. R.: The subsurface Palaeozoic stratigraphy of Southern Ontario, Ontario Geological Survey, Sudbury, Ontario., 2010.  
Chang, K. and Segall, P.: Injection induced seismicity on basement faults including poroelastic stressing, *Journal of Geophysical Research: Solid Earth*, 121(4), 2708–2726, 2016.
- 570 Dewers, T., Newell, P., Broome, S., Heath, J. and Bauer, S.: Geomechanical behavior of Cambrian Mount Simon Sandstone reservoir lithofacies, Iowa Shelf, USA, *International Journal of Greenhouse Gas Control*, 21, 33–48, doi:10.1016/j.ijggc.2013.11.010, 2014.  
Drenth, B. J., Anderson, R. R., Schulz, K. J., Feinberg, J. M., Chandler, V. W. and Cannon, W. F.: what lies beneath: geophysical mapping of a concealed Precambrian intrusive complex along the Iowa–Minnesota border, *Canadian Journal of Earth Sciences*, 52, 279–293, doi:10.1139/cjes-2014-0178, 2015.
- 575 Duffin, M. E., Lee, M., Klein, G. D. and Hay, R. L.: Potassic diagenesis of Cambrian sandstones and Precambrian granitic basement in UPH-3 deep hole, Upper Mississippi Valley, USA, *Journal of Sedimentary Research*, 59(5), 1989.  
Easton, R. M. and Carter, T. R.: Geology of the Precambrian basement beneath the Palaeozoic of southwestern Ontario, in *Basement Tectonics* 10, pp. 221–264, Springer., 1995.
- 580 Ellsworth, W. L., Llenos, A. L., McGarr, A. F., Michael, A. J., Rubinstein, J. L., Mueller, C. S., Petersen, M. D. and Calais, E.: Increasing seismicity in the U. S. midcontinent; implications for earthquake hazard (in Injection induced seismicity), *The Leading Edge*, 34(6), 618–626, 2015.  
Gilbert, R. C.: Final Report Minnesota Project (Area 4) Fillmore County, Minnesota, The New Jersey Zinc Company, Platteville Wisconsin., 1962.
- 585 Goebel, T. H. W. and Brodsky, E. E.: The spatial footprint of injection wells in a global compilation of induced earthquake sequences, *Science*, 361, 899–904, 2018.  
Hamblin, W. K.: The Cambrian sandstones of northern Michigan, University of Michigan., 1958.  
Hesseltine, G.: Micro to Macro Scale Structural and Lithological Architecture of Basal Nonconformities: Implications for Fluid Flow and Injection Induced Seismicity, MS, Utah State University, Logan, UT., 2019.
- 590 Keranen, K. M., H.M, S., G.A, A. and Cochran, E. S.: Potentially induced earthquakes in Oklahoma, USA: Links between wastewater injection and the 2011 Mw 5.7 earthquake sequence, *Geology*, 41(6), 699–702, 2013.  
Keranen, K. M., Weingarten, M., Abers, G. A., Bekins, B. A. and Ge, S.: Sharp increase in central Oklahoma seismicity since 2008 induced by massive wastewater injection, *Science*, 25, 448–451, 2014.
- 595 Kerner, K. R.: Permeability architecture of faulted nonconformities: Implications for induced seismicity, New Mexico Institute of Mining and Technology., 2015.  
Lemen, D., Lindline, J. and Bosbyshell, H.: The Gallinas Canyon gneiss: a window into the nature and timing of Paleoproterozoic events in Northern New Mexico, *Geology of the Las Vegas Region*., 2015.

- Lewan, M. D.: Metasomatism and weathering of the Presque Isle serpentinitized peridotite, Marquette, Michigan [MS thesis], 1972.
- 600 Marshak, S., Domrois, S., Abert, C., Larson, T., Pavlis, G., Hamburger, M., Yang, X., Gilbert, H. and Chen, C.: The basement revealed: Tectonic insight from a digital elevation model of the Great Unconformity, USA cratonic platform, *Geology*, 45(5), 391–394, doi:10.1130/G38875.1, 2017.
- Mossler, J. H.: *Geologic Atlas of Fillmore County, Minnesota*, University of Minnesota., 1995.
- 605 Murray, W. E.: *Class II Saltwater Disposal for 2009–2014 at the Annual, State, and County Scales by Geologic Zones of Completion*, Oklahoma, Oklahoma Geological Survey, Oklahoma., 2015.
- Nicholson, C. and Wesson, R. L.: *United States Geological Survey*, Alexandria, VA., 1990.
- Oliver, N. H. S., McLellan, J. G., Hobbs, B. E., Cleverly, J. S., Ord, A. and Feltrin, L.: Numerical models of extensional deformation, heat transfer, and fluid flow across basement-cover interfaces during basin-related mineralization, *Economic Geology*, 101(1), 1–31, 2006.
- 610 Ortiz, J. P.: *The role of fault zone architectural elements and basal altered zones on downward pore pressure propagation and induced seismicity in the crystalline basement*, New Mexico Institute of Mining and Technology, Socorro, New Mexico, USA., 2017.
- Ortiz, J. P., Person, M. A., Mozley, P. S., Evans, J. P. and Bilek, S. L.: The role of fault zone architectural elements on pore pressure propagation and induced seismicity, *Groundwater*, 57, 465–478, doi:10.1111/gwat.12818, 2019.
- 615 Petersen, M. D., Mueller, C. S., Moschetti, M. P., Hoover, S. M., Llenos, A. L., Ellsworth, W. L., Michael, A. J., Rubinstein, J. L., McGarr, A. F. and Rukstales, K. S.: 2016—One-year seismic hazard forecast for the Central and Eastern United States from induced and natural earthquakes., 2016.
- Rojstaczer, S. A. I. S. E. H. D. O.: Permeability of continental crust influenced by internal and external forcing, *Geofluids*, 8(2), 128–139, 2008.
- 620 Segall, P. and Lu, S.: Injection-induced seismicity: Poroelastic and earthquake nucleation effects, *Journal of Geophysical Research*, 120, 5280–5403, 2015.
- Sims, P. K.: *Precambrian Basement Map of the Northern Midcontinent*, U.S.A., 1990.
- Sloss, L. L.: *Sequences in the cratonic interior of North America*, 1963.
- 625 Smith, K., Paulding, A., Bradbury, K., Potter, K., Evans, J. and Petrie, E.: *Geologic Characterization of the Great Unconformity Injection Interface Region from Field and Drillcore Analog Studies: Implications for Midcontinent Induced Seismicity*, Phoenix, AZ, USA., 2019.
- Weingarten, M., Ge, S., Godt, J. W., Bekins, B. A. and Rubinstein, J. L.: High-rate injection is associated with the increase in U.S. mid-continent seismicity, *Science*, 248(6241), 1336–1340, 2015.
- 630 Whitmeyer, S. J. and Karlstrom, K. E.: Tectonic model for the Proterozoic growth of North America, *Geosphere*, 3(4), 220–259, 2007.

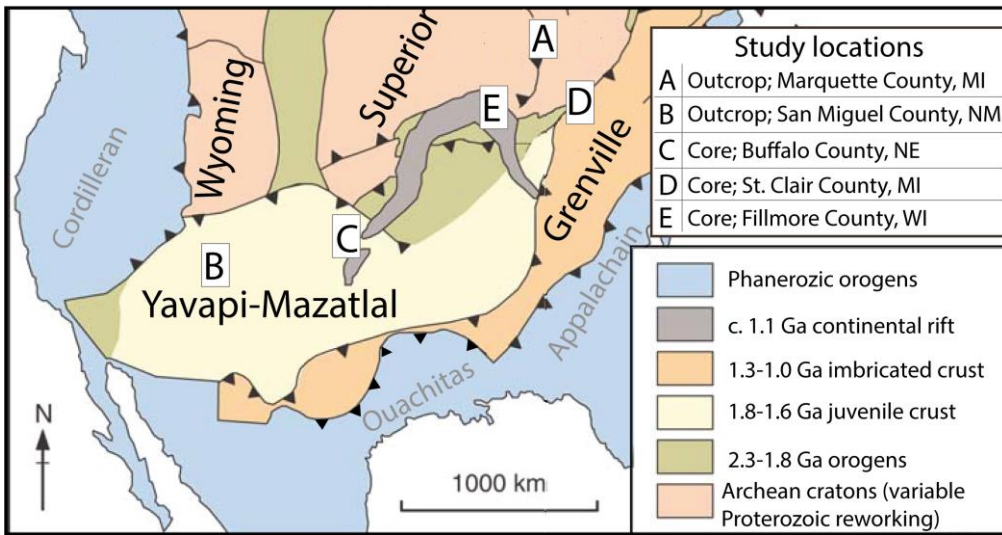
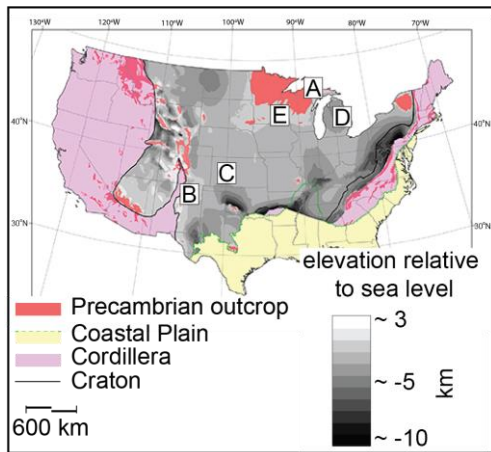
Wisconsin Geological Natural History Survey, Data: Porosity and density measurements: <https://wgnhs.wisc.edu/maps-data/data/rock-properties/porosity-density-measurements-data/>. Accessed August 2019

635 Yehya, A., Yang, Z. and Rice, J. R.: Effect of fault architecture and permeability evolution on response to fluid injection, *Journal of Geophysical Research: Solid Earth*, 123, 9982–9987, doi:10.1029/2018JB016550, 2018.

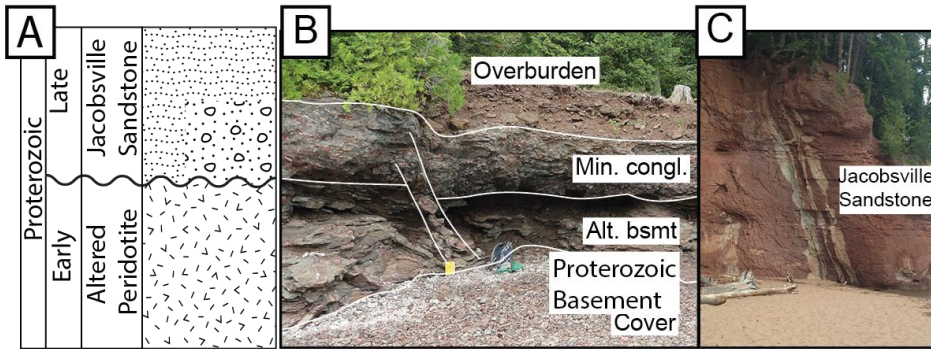
Zhang, Y., Person, M., Rupp, J., Ellett, K., Celia, M. A., Gable, C., Bowen, B., Evans, J., Bandilla, K., Mozley, P., Dewers, T. and Elliot, T.: Hydrogeologic Controls on Induced Seismicity in Crystalline Basement Rocks Due to Fluid Injection into Basal Reservoirs, *Groundwater*, doi:10.1111/gwat.12071, 2013.

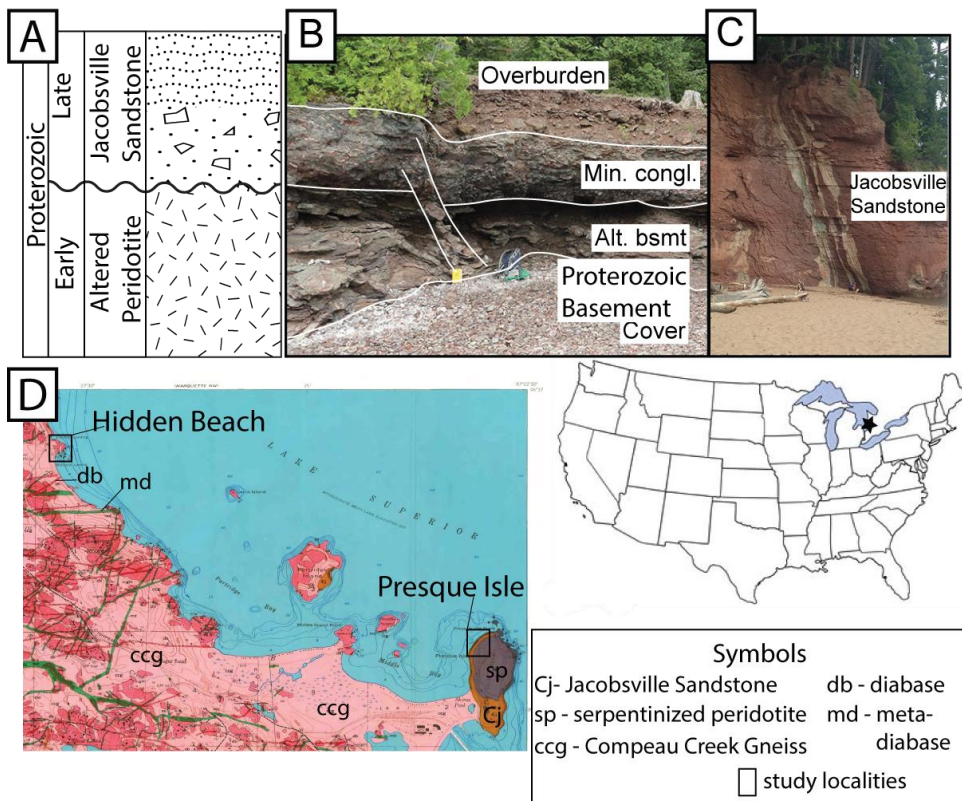
640 Zhang, Y., Edel, S. S., Pepin, J., Person, M., Broadhead, R., Ortiz, J. P., Bilek, S. L., Mozley, P. and Evans, J. P.: Exploring the potential linkages between oil field brine reinjection, crystalline basement permeability, and triggered seismicity for the Dagger Draw Oil field, southeastern New Mexico, USA, using hydrologic modeling, *Geofluids*, 16(5), 971–987, 2016.





645 Figure 1. Location of the nonconformity analogue study sites are noted on the top of basement digital elevation model (after Marshak et al., 2017). A) Lake Superior, Presque Isle, Michigan outcrop, B) Gallinas Canyon, New Mexico outcrop C) R.C. Taylor 1 core D) CPC BD-139 core and E) BO-1 core.





650 **Figure 2.** A) Schematic lithologic log at Lake Superior Michigan where altered peridotite is overlain by the Jacobsville Sandstone at Presque Isle and mineralized conglomerates of the Jacobsville Sandstone overlie the Compeau Gneiss at Hidden Beach. **Outcrop photos** B) Presque Isle and C) Hidden Beach outcrops. At this locality the Jacobsville Sandstone overlies the Proterozoic altered peridotite basement rocks. **D)** Geologic map of the Marquette, Michigan field area, showing locations of Hidden Beach and Presque Isle, modified from Gair and Thaden, 1968.

Formatted: Highlight

Commented [EP2]: Check text what are the basement rocks hidden beach

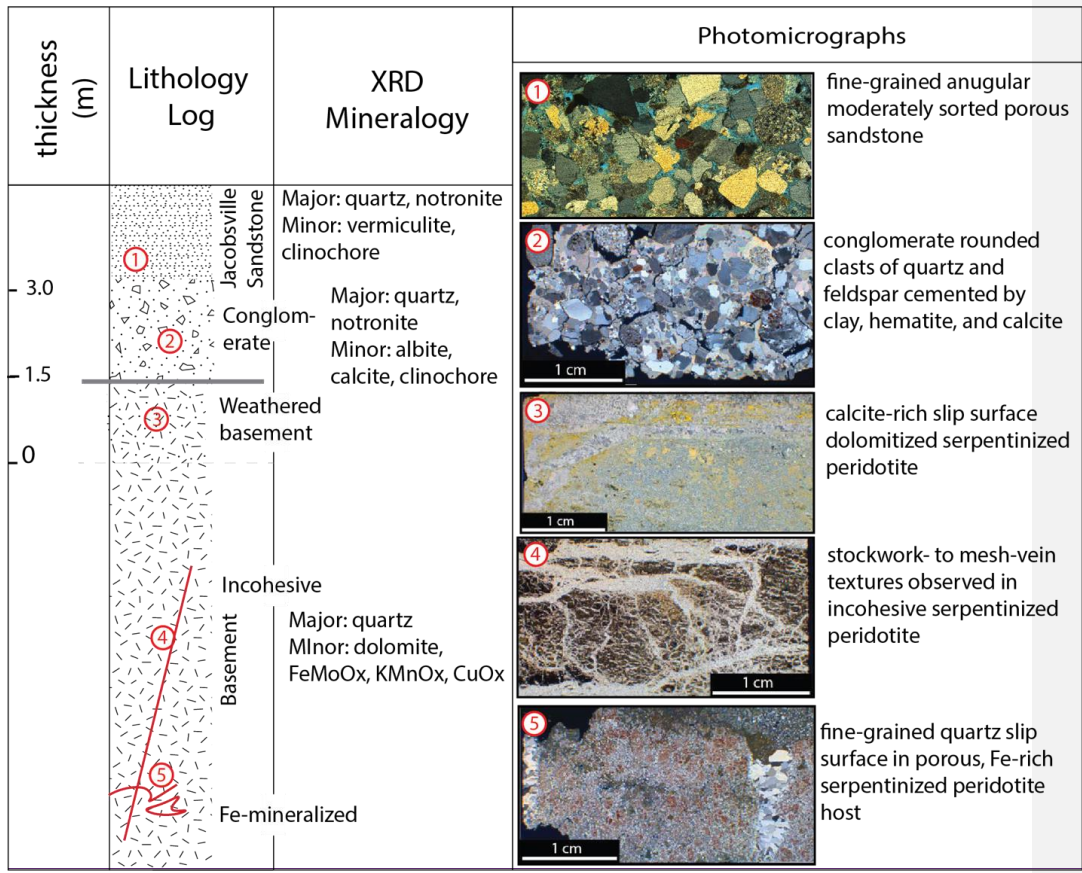
Formatted: Highlight

Formatted: Font: 10 pt, Highlight

Formatted: Font: 10 pt

Formatted: Font: 9 pt

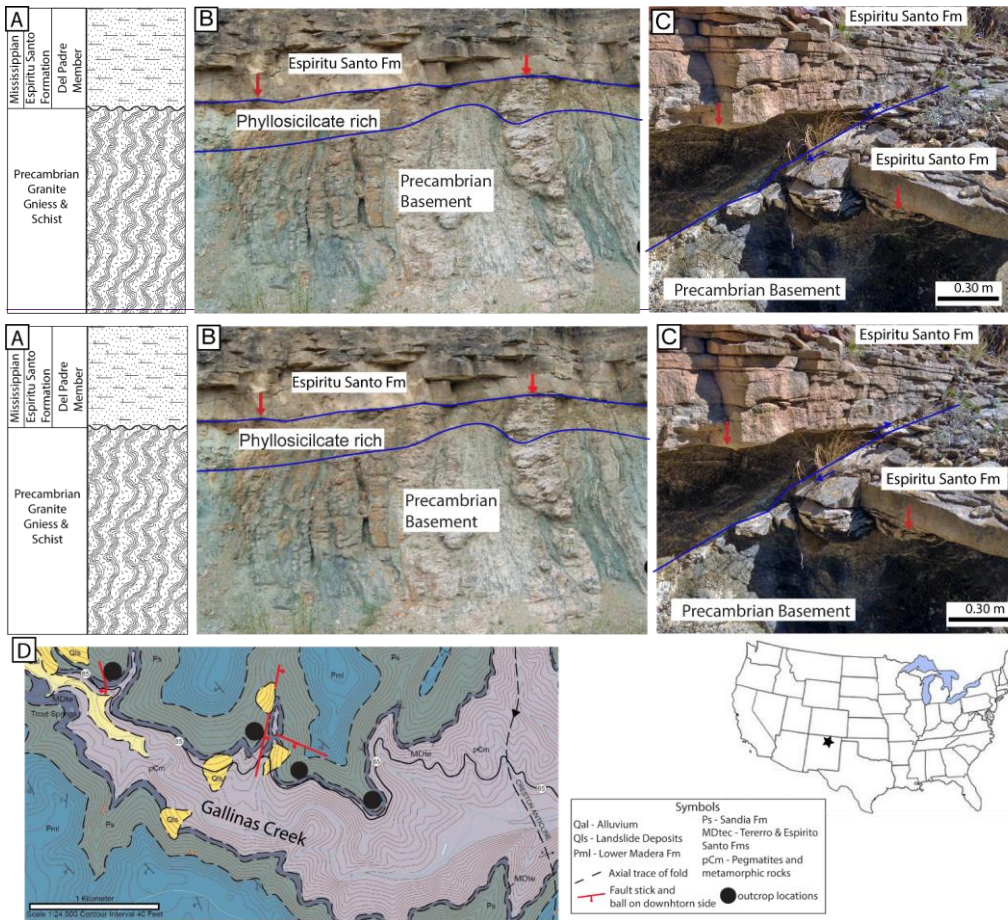
Formatted: Font: 9 pt



655

Figure 3. Petrographic summary figure, photomicrographs and X-ray diffraction results of nonconformity units studied at Presque Isle, Michigan. 1) Jacobsville Sandstone arenite (100x, ppl) 2) Jacobsville Sandstone altered conglomerate (200x, ppl), 3) Basement calcite-rich slip surface in dolomitized, serpentinized peridotite (200x, xpl), B) Basement serpentine (100x, ppl), C) Basement slip surface within cataclasis and associated colloform mineralization (100x, ppl), D) Basement vein assemblages (200x, xpl).

660



665

**Figure 3.** A) Gallinas Canyon, New Mexico outcrop lithology log. B) Precambrian granitic gneiss and schist is overlain by the Mississippian Espiritu Santo Formation, red arrows mark the nonconformity, blue lines mark boundary of phyllosilicate alteration. C) The 4 km long exposure in Gallinas Canyon, the nonconformity is cut by several cm- to m- displacement faults, red arrows mark the nonconformity, fault shown by green line. D) Geologic map of Gallinas Canyon study area, modified from Hesselstine, 2019. Faults that cut the nonconformity are shown in red with ball on down dropped, at map scale the nonconformity is relatively planar, and parallels topographic contour lines.

Figure 4. Gallinas Canyon, New Mexico outcrop, Precambrian granitic gneiss and schist is overlain by the Mississippian Espiritu Santo Formation. The 4 km long exposure in Gallinas Canyon, the nonconformity is cut by several cm- to m- displacement faults (C).

Formatted: Left, Line spacing: single, Don't adjust space between Latin and Asian text, Don't adjust space between Asian text and numbers

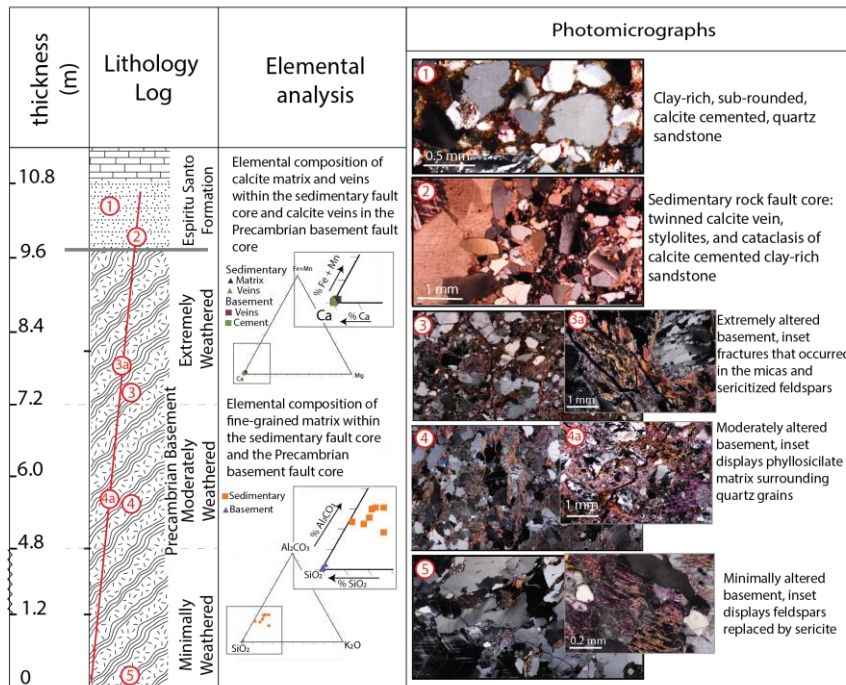
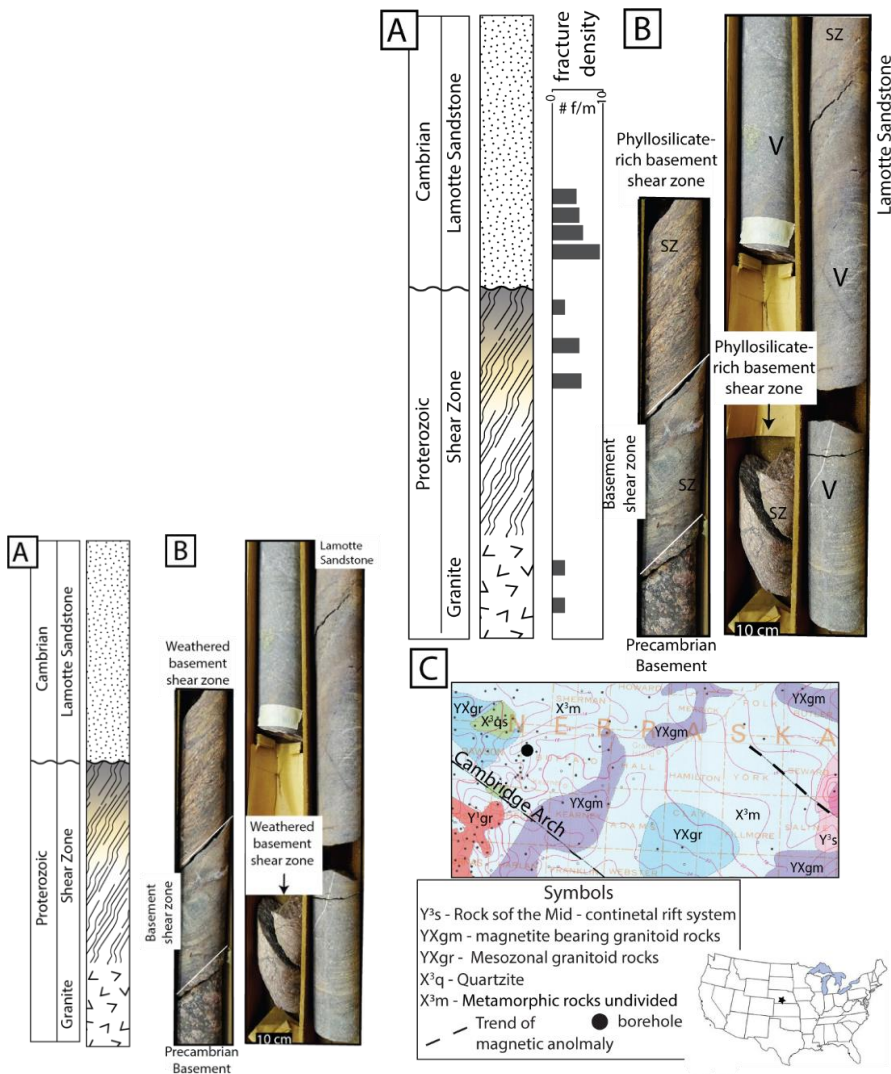


Figure 5. Petrographic and elemental analysis summary of nonconformity units at Gallinas Canyon site. Elemental analysis shows similar calcite composition of the veins within the sedimentary sequence and the Precambrian basement faults. 1 & 2) The Espiritu Santo sandstones are clay rich calcite cemented quartz sandstones, in the fault core (2) the sandstones are cut by twinned calcite veins and stylolitic textures and contact cataclastic; 3) adjacent to the nonconformity the granitic basement contain fractures in the micas and sericitized feldspars; 4) & 5) basement alteration decreases away from the nonconformity with phyllosilicate matrix surrounding quartz grains and sericitization of feldspars occurring 10 m from the nonconformity.



**Figure 4.** A) Lithologic log of the R.C. Taylor 1 core, Nebraska, core from 3984-4038' (1214-1231 m) measured depth. The nonconformity occurs at 4018' MD (1225 m). Fracture density in core is based on number of fractures per meter of core. Four lithologic units are identified in the core, including sandstone, sedimentary rock hosted shear zone, altered basement shear zone,

minimally altered basement. The nonconformity occurs between the altered basement shear zone and overlying sandstone of the La Motte Formation. B) Photographs of the R.C. Taylor 1 core. Both the basement shear zone (SZ) and overlying sandstone are cut by veins (V) of quartz, calcite and Fe-oxides. C) Borehole location shown on the Precambrian basement map from Sims (1990).

685 Figure 6. A) Lithologic log of the R.C. Taylor 1 core, Nebraska, core from 3984-4038' (1214-1231 m) was described. The nonconformity occurs at 4018' MD (1225 m). Four main lithologic units were defined in the core, including sandstone, sedimentary rock hosted shear zone, altered basement shear zone, minimally altered basement. The nonconformity occurs within a shear zone and is cut by thoroughgoing veins.

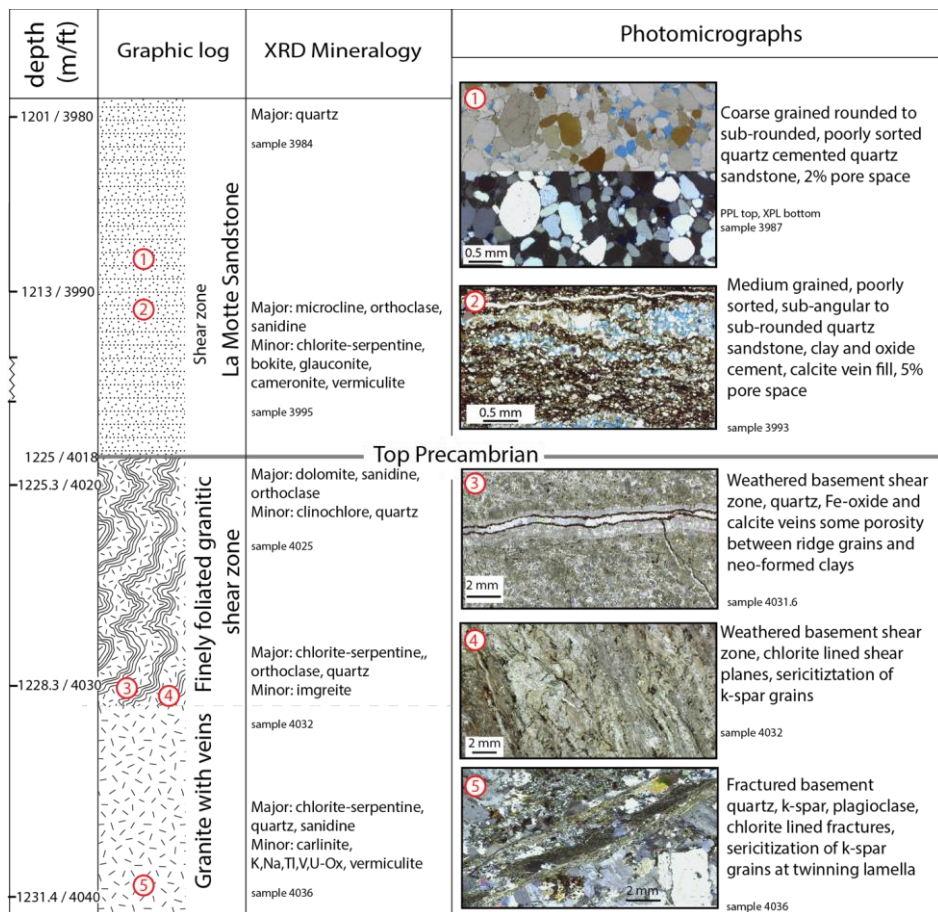




Figure 7. Petrographic summary figure, photomicrographs and X-ray diffraction results of nonconformity units studied in the R.C. Taylor 1 core; 1) Lamotte Sandstone, rounded to sub-rounded, poorly sorted quartz sandstones (100x, ppl & xpl); 2) lower Lamotte Sandstone, opaque Fe-oxide cements and vein fill, porosity shown by blue epoxy, (100x ppl); 3) Top Precambrian crystalline altered basement shear zone. Syntaxial veins mineralized with quartz, reactivated and mineralized with Fe-oxide then sparry calcite. Some porosity between rigid grains and neo-formed clays (50x PPL); 4) Altered basement shear zone, chlorite lined shear planes, sericitization of feldspars along twinning lamella (100x ppl); 5) Coarse crystalline sericitization of feldspars adjacent to twin lamellae (150x XPL).

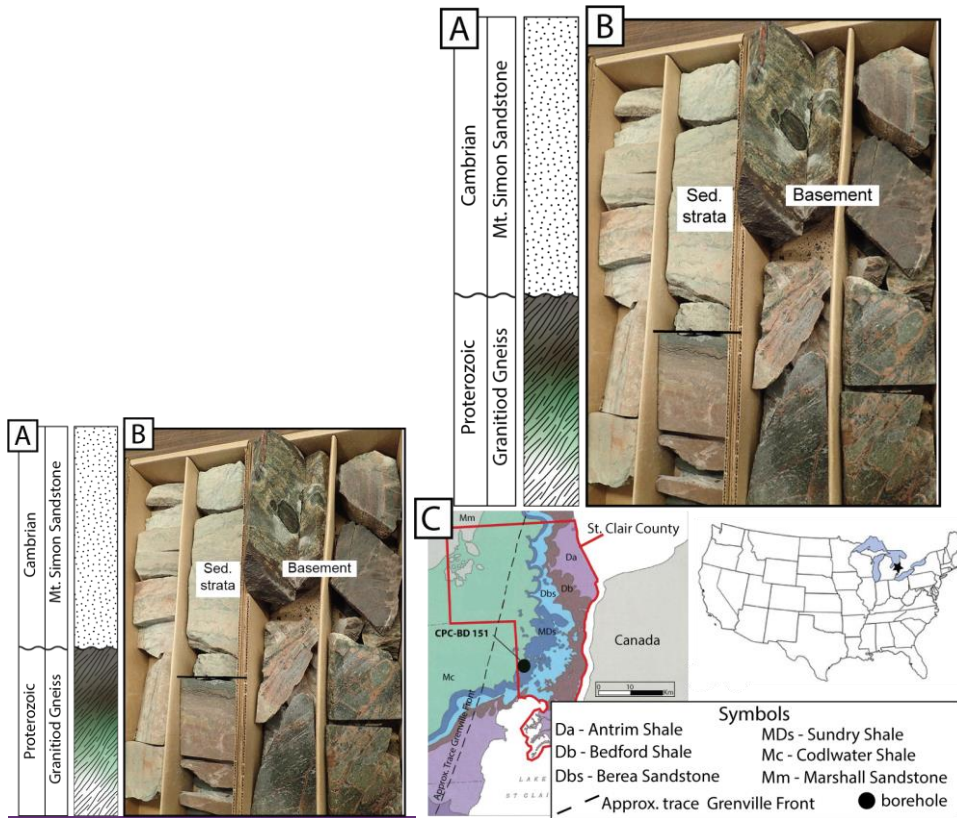


Figure 5. A) Lithologic log of the CPC BD-139 core, Michigan from 1404-1412.1 meters measured depth. Five main lithologic units identified, including sandstone, dolomitized and undolomitized finely foliated gneiss, and dolomitized and undolomitized gneiss with sub-horizontal white veins. B) Photographs of the CPC BD-139 core. Core between -1404.5-1405.5 meters. Contact between the Cambrian Mount Simon Sandstone (light tan) and the underlying Precambrian gneiss. The gneiss directly at the contact is fine-

grained, tan, and dolomitized. This is underlain by green altered gneiss with sub-vertical pink fractures. This lithology grades into a dark grey gneiss with sub-horizontal white veins (core between 1411.5-1412.5 meters), which extends through the bottom of the logged section. C) Geologic map St. Clair County, Michigan, modified from Milstein, (1987).

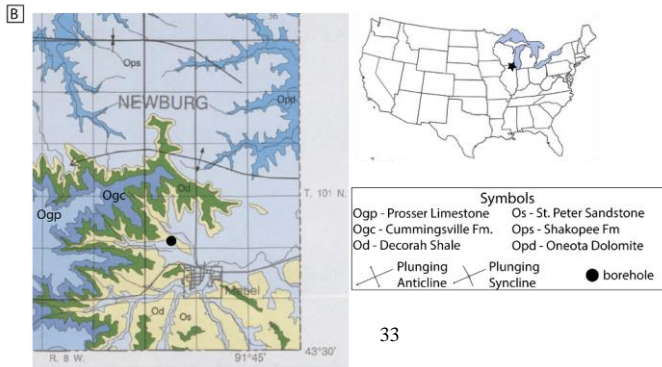
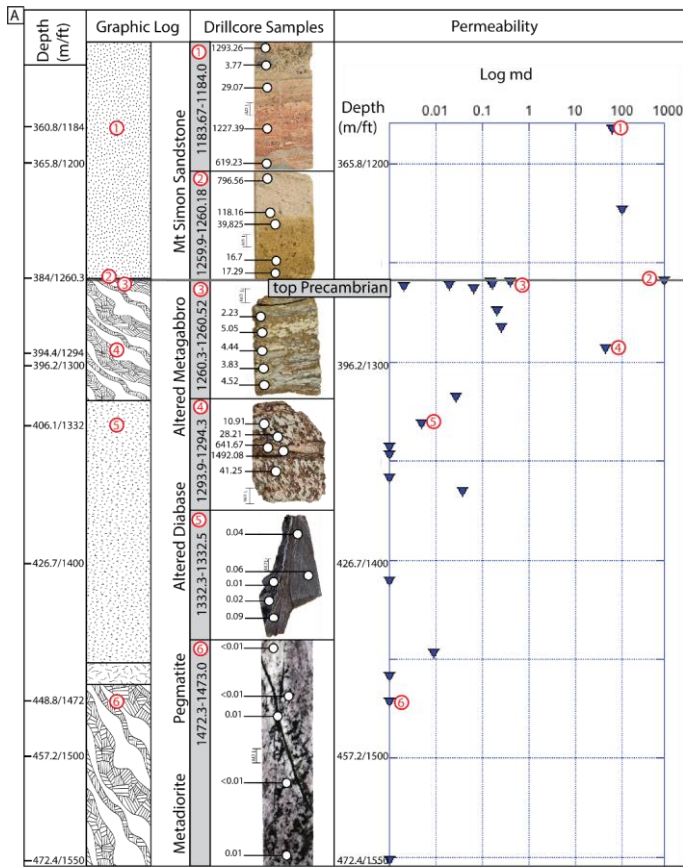
705

Figure 8. A) Lithologic log of the CPC BD-139 core, Michigan from 1404-1412.1 meters depth. Five main lithologic units were identified, including sandstone, dolomitized and undolomitized finely foliated gneiss, and dolomitized and undolomitized gneiss with sub-horizontal white veins. B) Photographs of the CPC BD-139 core. Core between ~1404.5-1405.5 meters. Contact between the Cambrian Mt. Simon Sandstone (light tan) and the underlying Precambrian gneiss. The gneiss directly at the contact is fine-grained,

710

tan, and dolomitized. This is underlain by green altered gneiss with sub-vertical pink-coated fractures. This lithology grades into a

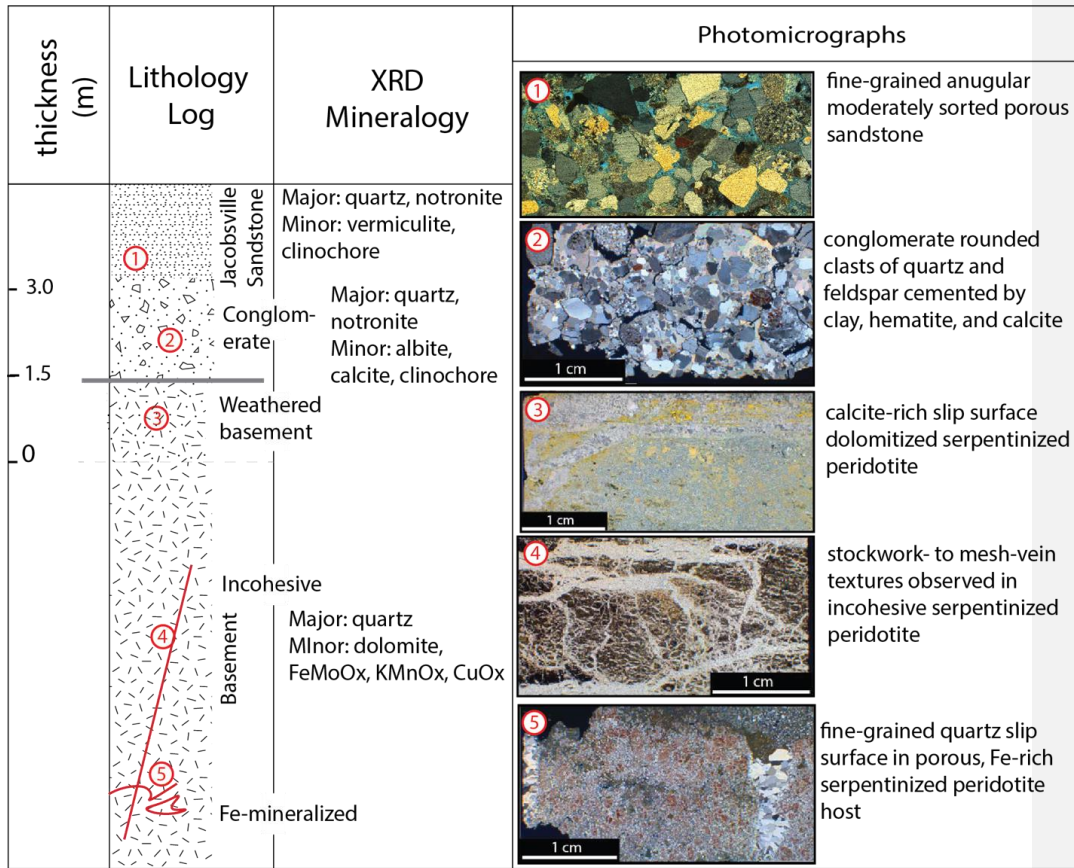
dark grey gneiss with sub-horizontal white veins (core between 1411.5-1412.5 meters), which extends through the bottom of the



logged section.

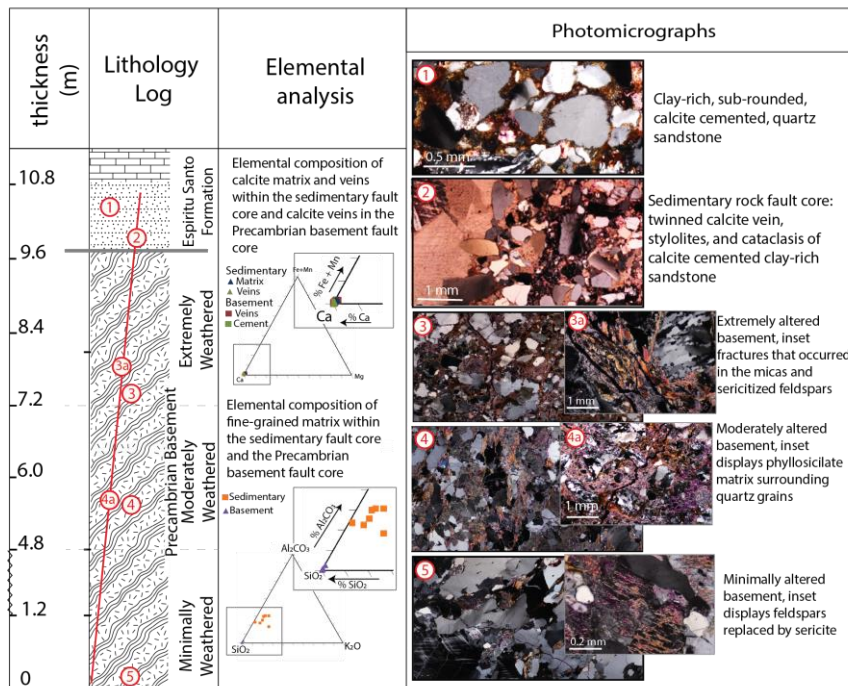
715 **Figure 6. A) BO-1 lithologic log with select representative core samples of each the major lithologic units. Above the nonconformity, the analogue reservoir or injection unit, the Cambrian Mount Simon Sandstone is porous with evidence for both dissolution and oxidation front. The crystalline basement rock consists of foliated, intensely altered and altered metagabbro with localized faulting, variably altered and faulted diabase localized intrusions, pegmatite dikes, and at greater depths, relatively unaltered and less-deformed metadiorite. Gas permeability measurements were made on 25 core samples spanning the nonconformity interface. For each core sample tested, 5 spot measurements were made (locations shown by white circles). For relative comparison across the contact and within the various lithologic units, data is plotted using a log scale and the averaged values for each sample. B) Geologic map modified from Mossler, et al., 1995.**

720



**Figure 7. Petrographic summary figure, photomicrographs and X-ray diffraction results of nonconformity units studied at Presque Isle, Michigan. 1) Jacobsville Sandstone arenite (100x, ppl) 2) Jacobsville Sandstone altered conglomerate (200x, ppl), 3) Basement calcite-rich slip surface in dolomitized, serpentinized peridotite (200x, xpl), 4) Basement serpentinized peridotite (100x, ppl), 5) Basement slip surface within in Fe-rich serpentinized peridotite (red) (100x, ppl).**

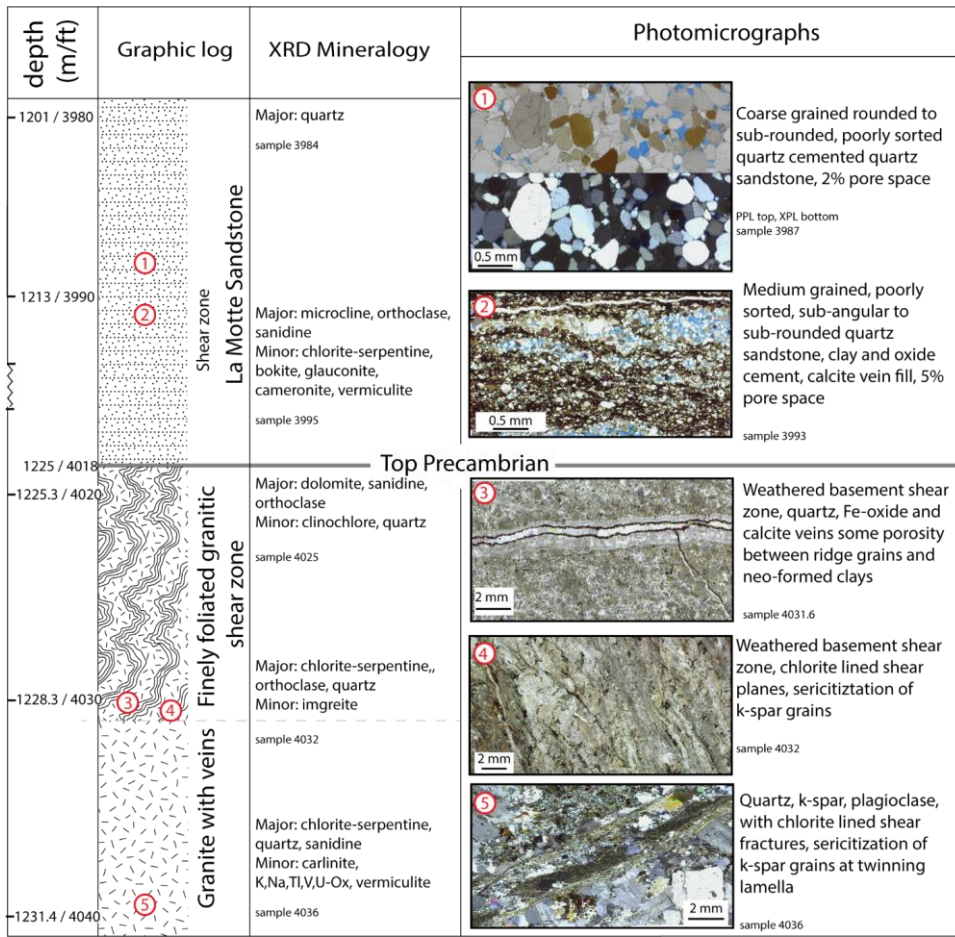
725



**Figure 8. Petrographic and elemental analysis summary of nonconformity units at Gallinas Canyon site. Thickness is measured in meters from base of outcrop section, red line represents fault. Elemental analysis shows similar calcite composition of the veins within the sedimentary sequence and the Precambrian basement faults. 1 & 2) The Espiritu Santo sandstones are clay rich calcite cemented quartz sandstones, in the fault core, 2) the sandstones are cut by twinned calcite veins and stylolitic textures and contact cataclastic; 3) adjacent to the nonconformity the granitic basement contain fractures in the micas and sericitized feldspars; 4) & 5) basement alteration decreases away from the nonconformity with phyllosilicate matrix surrounding quartz grains and sericitization of feldspars occurring 10 m from the nonconformity.**

730

735



**Figure 9. Petrographic summary figure, photomicrographs and X-ray diffraction results of nonconformity units studied in the R.C. Taylor 1 core; 1) La Motte Formation sandstone, rounded to sub-rounded, poorly sorted quartz sandstones (100x, ppl & xpl); 2) lower La Motte Formation, opaque Fe-oxide cements and vein fill, porosity shown by blue epoxy, (100x ppl); 3) Top Precambrian crystalline altered basement shear zone. Syntaxial veins mineralized with quartz, reactivated and mineralized with Fe-oxide then sparry calcite. Some porosity between rigid grains and neo-formed clays (50x PPL); 4) Altered basement shear zone, chlorite lined**

shear planes, sericitization of feldspars along twining lamella (100x ppl); 5) Coarse crystalline sericitization of feldspars adjacent to twin lamellae (150x XPL).

745

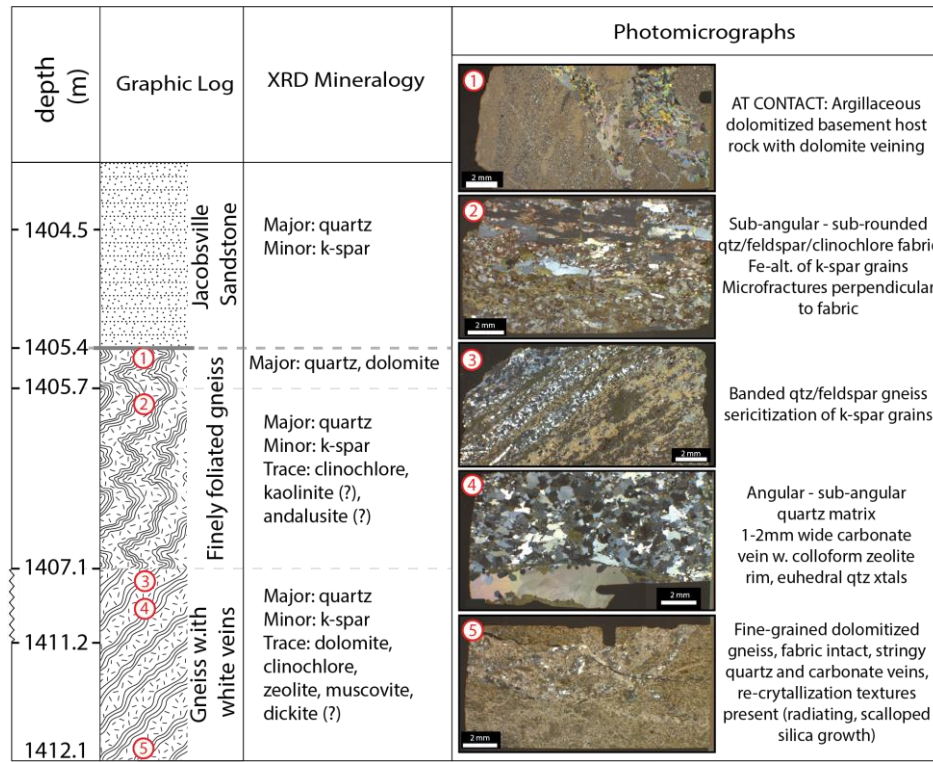


Figure 10. Petrographic summary figure, depth in meters measured depth, photomicrographs and X-ray diffraction results of nonconformity units studied in CPC BD-139 core. 1) Basement sample at the contact is an argillaceous dolomitized gneiss with dolomite veins (XPL); 2) Foliation defined by quartz-feldspar-clinochlore fabric with iron alteration of potassium feldspar grains (XPL); 3) banded quartz-feldspar gneiss with common sericitization of potassium feldspar grains (XPL); 4) Carbonate vein with colloform zeolite rim and euhedral quartz crystals (XPL); 5) dolomitized gneiss with common quartz and carbonate veins (XPL).

750



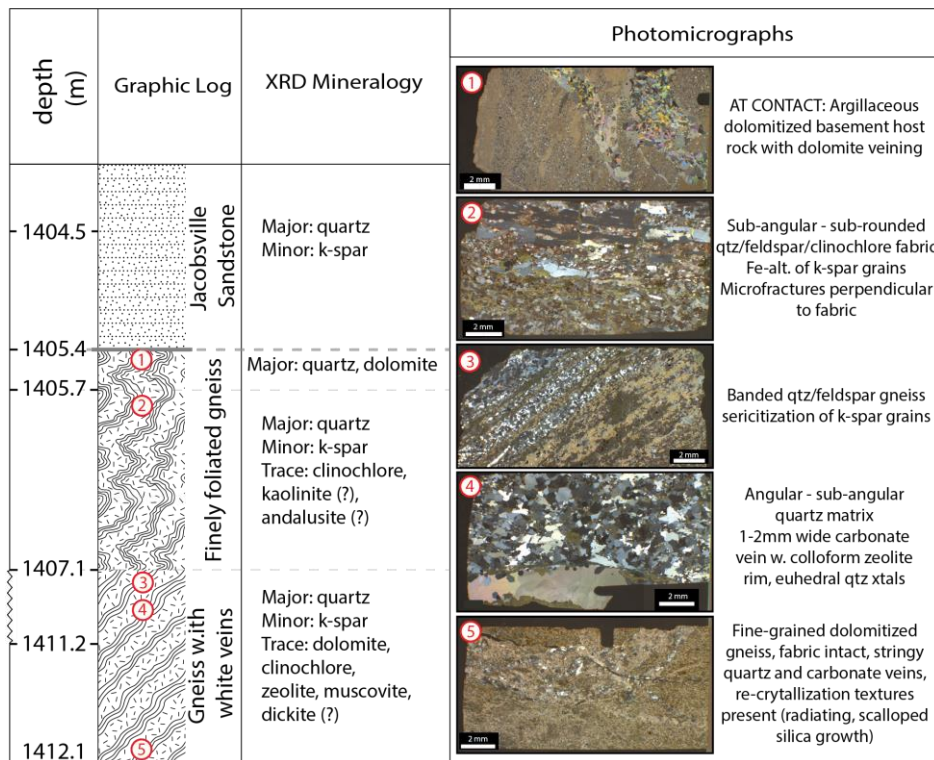


Figure 9. Petrographic summary figure, photomicrographs and X-ray diffraction results of nonconformity units studied in CPC BD-139 core. 1) Basement sample at the contact is an argillaceous dolomitized gneiss with dolomite veins (XPL); 2) Foliation defined by quartz-feldspar-clinochlore fabric with iron alteration of potassium feldspar grains (XPL); 3) banded quartz-feldspar gneiss with common sericitization of potassium feldspar grains (XPL); 4) Carbonate vein with colloform zeolite rim and euhedral quartz crystals (XPL); 5) dolomitized gneiss with common quartz and carbonate veins (XPL).

755

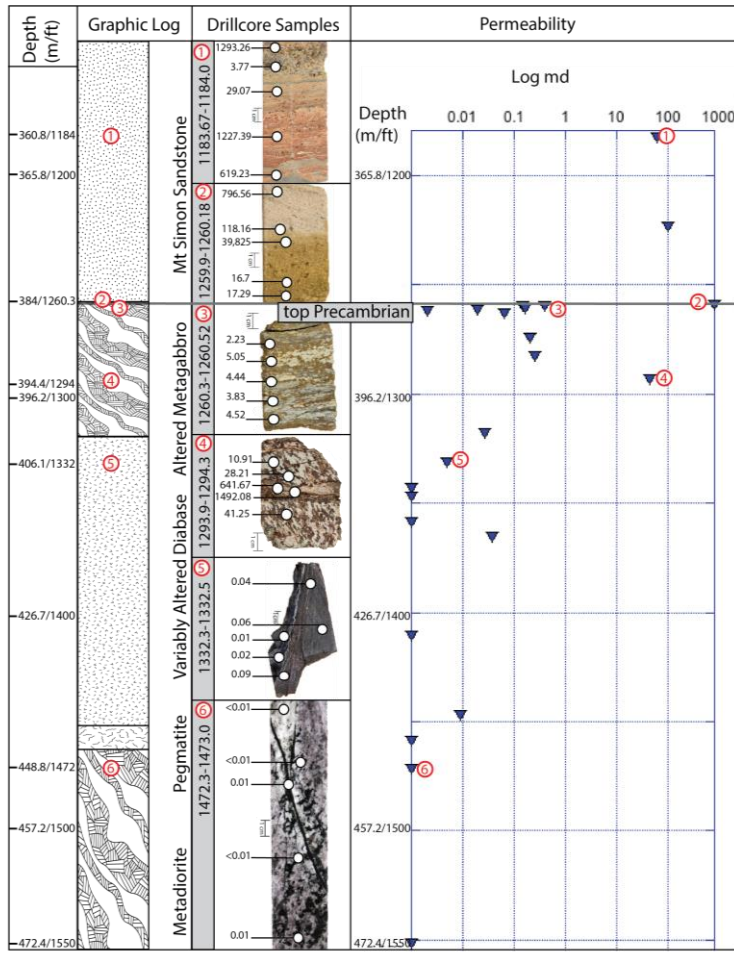
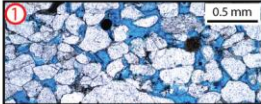
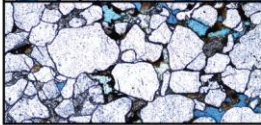
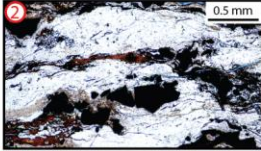
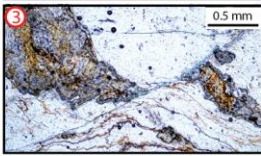
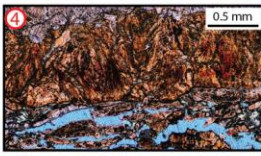

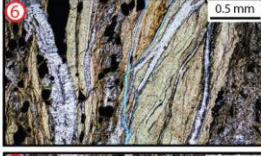



Figure 10. BO-1 lithologic log with select representative core samples of each the major lithologic units shown. Above the nonconformity, the analogue reservoir or injection unit, the Cambrian Mt. Simon Sandstone is porous with evidence for both dissolution and oxidation front. The crystalline basement rock consists of foliated, intensely altered and altered metagabbro with localized faulting, variably altered and faulted diabase, localized pegmatite dikes, and relatively unaltered and less-deformed metadiorite. **Gas permeability measurements were made on 25 core samples spanning the nonconformity interface. For each core**

Formatted: Highlight

765 **sample tested, 5 spot measurements per sample. Results shown by lithologic unit.** For relative comparison across the contact and within the various lithologic units, data is plotted using a log scale and the averaged values for each sample.

Depth (m/ft)	Graphic Log	XRD Mineralogy	Photomicrographs	
			Image	Description
365.8/1200	Mt Simon Sandstone	Major: quartz Minor: Fe-oxides		fine- to medium-grained, subangular to subrounded, well-sorted porous sandstone
		Major: quartz, Fe-oxides Minor: Fe-hydroxide (goethite)		iron-coated and irregularly cemented, siderite crystals partially fill pore space Sample: 1259.9-1260.18
<b>Nonconformity contact</b>				
384.4/1260.3	Altered Metagabbro	Major: Fe-hydroxide (goethite), Mn-oxides, Fe-oxides, magnesio-chloritoid (ferroan) Minor: ankerite, dolomite		strongly weathered, meta-gabbro-norite intensely altered ~ 60 m dolomitization Sample: 1260.3-1260.52
394.4/1294 396.2/1300 398/1305.9		HOST Major: dolomite, Ti-oxide (anatase) Minor: ramsbeckite SLIP Major: dolomite, birnessite, Mo-oxide, quartz, nacrite clay (kaolinite-serpentine)		argillization-alteration along discrete discontinuities multiple cm - micrometer scale slip surfaces Sample: 1260.52-1261.25
406.1/1332	Variably Altered Diabase	Major: Fe-oxides, Cu-hydroxides (clinoclase), muscovite, illite		argillization-alteration extends outward from fracture surfaces open fractures Sample: 1293.9-1294.3
426.7/1400		HOST Major: siderite, dolomite, adularia minor: Fe-rich smectite (nontronite)		multi-layered vein, slip surface dilational pull-apart micro-structures crack-seal textures serpentinization, dolomitization Sample: 1305.85-1305.95
448.8/1472	Pegmatite	HOST Major: diopside, clinoclase (Fe-rich) Minor: Mn-oxides, andesine, ramsbeckite SLIP Major: quartz, Fe-oxides Minor: fluorapatite, zeolites, Mn-oxides		multi-layered shear zone of multi-phase composition anastomosing and cross-cutting vein textures Sample: 1332.3-1332.5
457.2/1500		Metadiorite	Major: albite (Ca), anorthite, Minor: calcite, ferro-actinolite, vermiculite, Na-Ca plagioclase (andesine)	

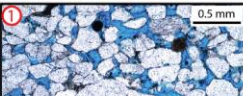

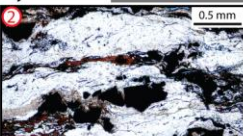
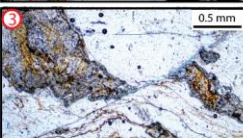

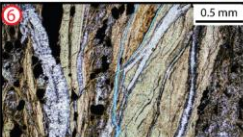
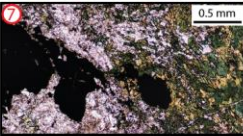
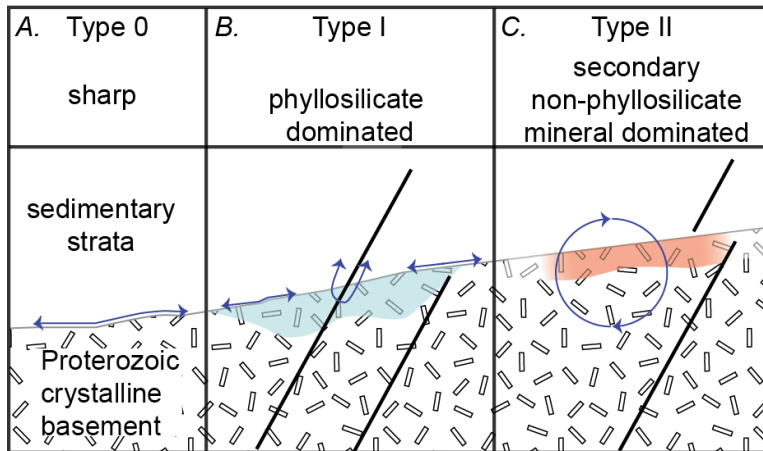
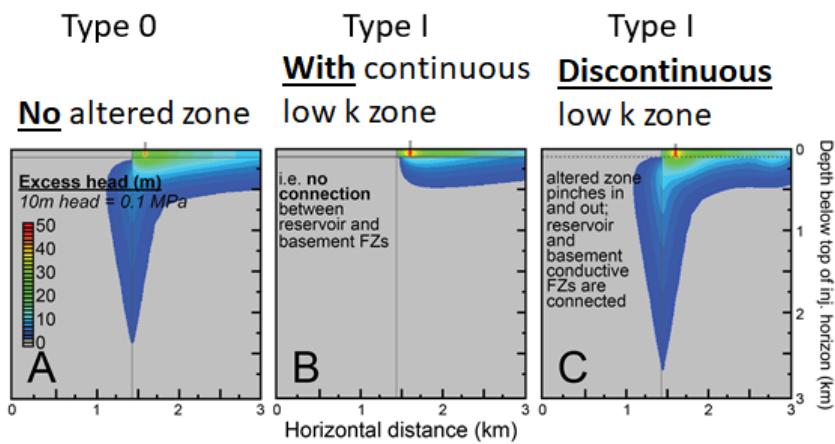
Depth (m/ft)	Graphic Log	XRD Mineralogy	Photomicrographs
365.8/1200	Mount Simon Sandstone	Major: quartz Minor: Fe-oxides	 <p>fine- to medium-grained, subangular to subrounded, well-sorted porous sandstone</p>
		Major: quartz, Fe-oxides Minor: Fe-hydroxide (goethite)	 <p>iron-coated and irregularly cemented, siderite crystals partially fill pore space</p> <p>Sample: 1259.9-1260.18</p>
384/1260.3	<b>Nonconformity contact</b>		
	Altered Metagabbro	Major: Fe-hydroxide (goethite), Mn-oxides, Fe-oxides, magnesio-chloritoid (ferroan) Minor: ankerite, dolomite	 <p>altered meta-gabbro-norite with dolomitization</p> <p>Sample: 1260.3-1260.52</p>
394.4/1294 396.2/1300 398/1305.9		HOST Major: dolomite, Ti-oxide (anatase) Minor: ramsbeckite SLIP Major: dolomite, birnessite, Mo-oxide, quartz, nacrite clay (kaolinite-serpentine)	 <p>argillization along discrete discontinuities</p> <p>multiple cm - micrometer scale slip surfaces</p> <p>Sample: 1260.52-1261.25</p>
406.1/1332		Variably Altered Diabase	Major: Fe-oxides, Cu-hydroxides (clinoclase), muscovite, illite
426.7/1400	Pegmatite	HOST Major: siderite, dolomite, adularia Minor: Fe-rich smectite (nontronite)	 <p>multi-layered vein, slip surface dilational pull-apart microstructures</p> <p>crack-seal textures</p> <p>serpentinization, dolomitization</p> <p>Sample: 1305.85-1305.95</p>
		HOST Major: diopside, clinoclase (Fe-rich) Minor: Mn-oxides, andesine, ramsbeckite SLIP Major: quartz, Fe-oxides Minor: fluorapatite, zeolites, Mn-oxides	 <p>multi-layered shear zone of multi-phase composition</p> <p>anastomosing and cross-cutting vein textures</p> <p>Sample: 1332.3-1332.5</p>
448.8/1472	Metadiorite	Major: albite (Ca), anorthite, Minor: calcite, ferro-actinolite, vermiculite, Na-Ca plagioclase (andesine)	 <p>moderately altered feldspars</p> <p>ultracataclase along mm-scale shear zones</p> <p>Sample: 1472.3-1473</p>
457.2/1500			

Figure 11. X-ray Diffraction mineralogy and photomicrographs of BO-1 drill core samples showing representative compositions and textures across the non-conformity interface contact. Samples within centimetres of the contact (1-3) are strongly weathered, altered, and slightly metamorphosed gabbro-norite. Alteration and diagenesis assemblages include iron-oxides-hydroxides with chlorite, ankerite, and dolomite. Alteration extends for ~ 50 m into the basement. Sample 3 illustrates mm-scale offset across argillite layer. Note fracture permeability (blue-epoxy) parallel to slip surface. Fracture surfaces within Sample 4 at 34 m below the contact are several mm's of mixed chlorite-clay alteration and fine-scale permeability (blue-epoxy). Sample 5 at 1304.9 m shows multiple phases of fluid-rock interactions coupled with dilation, serpentinization, and dolomitization. Multi-layered clay-rich fault core gouge within Sample 6 at 1332 m or ~ 70 m below the contact. Note, open fractures within central portion of fault core gouge (blue-epoxy). At 1472 m or 272 m below the contact within the meta-grano-diorite unit, clay alteration is observed within feldspar grains at the micro-scale.

Figure 11. X-ray Diffraction mineralogy and photomicrographs of BO-1 drill core samples showing representative compositions and textures across the non-conformity interface contact. Samples within centimetres of the contact (1-3) are strongly weathered, altered, and slightly metamorphosed gabbro-norite. Alteration and diagenesis assemblages include Iron-oxides-hydroxides with chlorite, ankerite, and dolomite. Alteration extends for ~ 50 m into the basement. Sample 3 illustrates mm-scale offset across argillite layer. Note fracture permeability (blue-epoxy) parallel to slip surface. Fracture surfaces within Sample 4 at 34 m below the contact are several mm's of mixed chlorite-clay alteration and fine-scale permeability (blue-epoxy). Sample 5 at 1304.9 m shows multiple phases of fluid-rock interactions coupled with dilation, serpentinization, and dolomitization. Multi-layered clay-rich fault core gouge within Sample 6 at 1332 m or ~ 70 m below the contact. Note, open fractures within central portion of fault core gouge (blue-epoxy). At 1472 m or 272 m below the contact within the meta-grano-diorite unit, clay alteration is observed within feldspar grains at the micro-scale.

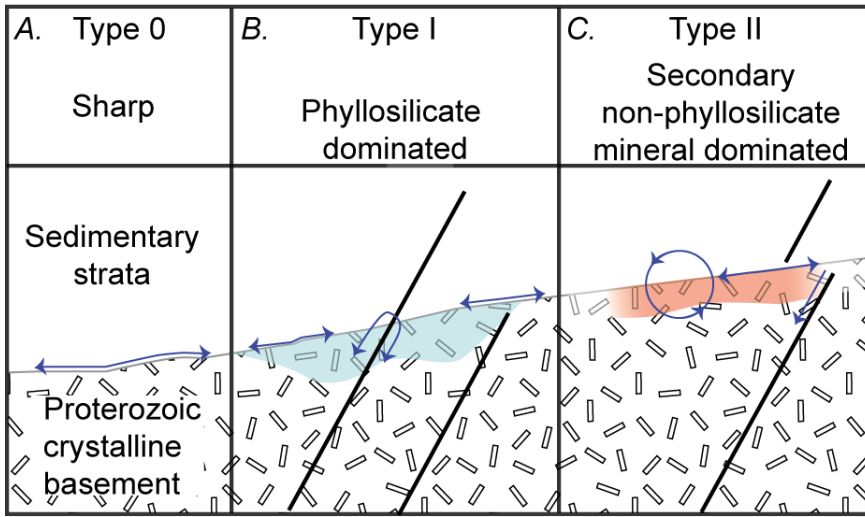


790 Figure 12. Proposed geologic schematics of the non-conformity contact region. A. Type 0 — sharp contact; B. Type I — weathering dominated zone Proterozoic crystalline basement, C. Type II — secondary mineralization dominated zone. All nonconformity types may be cut by structural discontinuities. Blue arrows indicate potential flow paths of injected fluids.



795 Figure 13. Cross-sectional views of pore pressure envelope propagation resulting from injection into a reservoir underlain by a low permeability altered zone. Excess hydraulic heads after 4 years of constant-rate injection are presented for a Palaeozoic conduit-barrier fault scenario (A) Type 0 nonconformity, absent a low-permeability altered zone, (B) Type I nonconformity, with an altered zone present as a 20-m-thick confining layer (represented by two horizontal grey lines) that is continuous such that reservoir and basement fault zones do not connect, and (C) Type I nonconformity, with a discontinuous altered zone that pinches in and out in 20-m horizontal intervals (i.e. undulating) but where the reservoir and basement fault zones are fully connected. Results are zoomed in to the top 3 km × 3 km of the model domain. Vertical grey lines indicate location of the fault zone. Injection well location is indicated on top of each panel. Transition from grey to dark blue contour (and all subsequent contour lines) denotes a 2-m increase in hydraulic head (0.02 MPa). Adapted from Ortiz (2017; for details of the modelling approach see Ortiz et al., 2019).

800



805 Figure 13. Proposed geologic schematics of the non-conformity contact region. A) Type 0 – sharp contact expected to prevent direct fluid pressure communication across the contact while promoting migration parallel to the contact distributing fluids laterally; B) Type I – phyllosilicate dominated zone above crystalline basement is expected to inhibit fracture propagation across the nonconformity, prevent fluid migration due to permeability contrast and promote lateral migration; downward fluid migration can occur at a permeable fault zone; C) Type II – secondary mineralization dominated zone, lateral migration due to permeability contrast, mineralization due to fluid-rock interactions suggests that deep fluid circulation occurs even without enhanced permeability from fractures. All nonconformity types may be cut by structural discontinuities. Blue arrows indicate potential flow paths of injected fluids.

810

Table 1. Nonconformity type and sample location.

<u>Nonconformity type</u>	<u>Location</u>
Type 0 - sharp contact	Hidden Beach Marquette, Michigan
Type I – altered contact phyllosilicate mineralization	Gallinas Canyon, New Mexico RC Taylor Core
Type II – altered contact, non-phyllosilicate secondary mineralization	Presque Isle, Marquette, Michigan CPC BD-139 Core BO Core

815

Formatted: Font: Not Bold